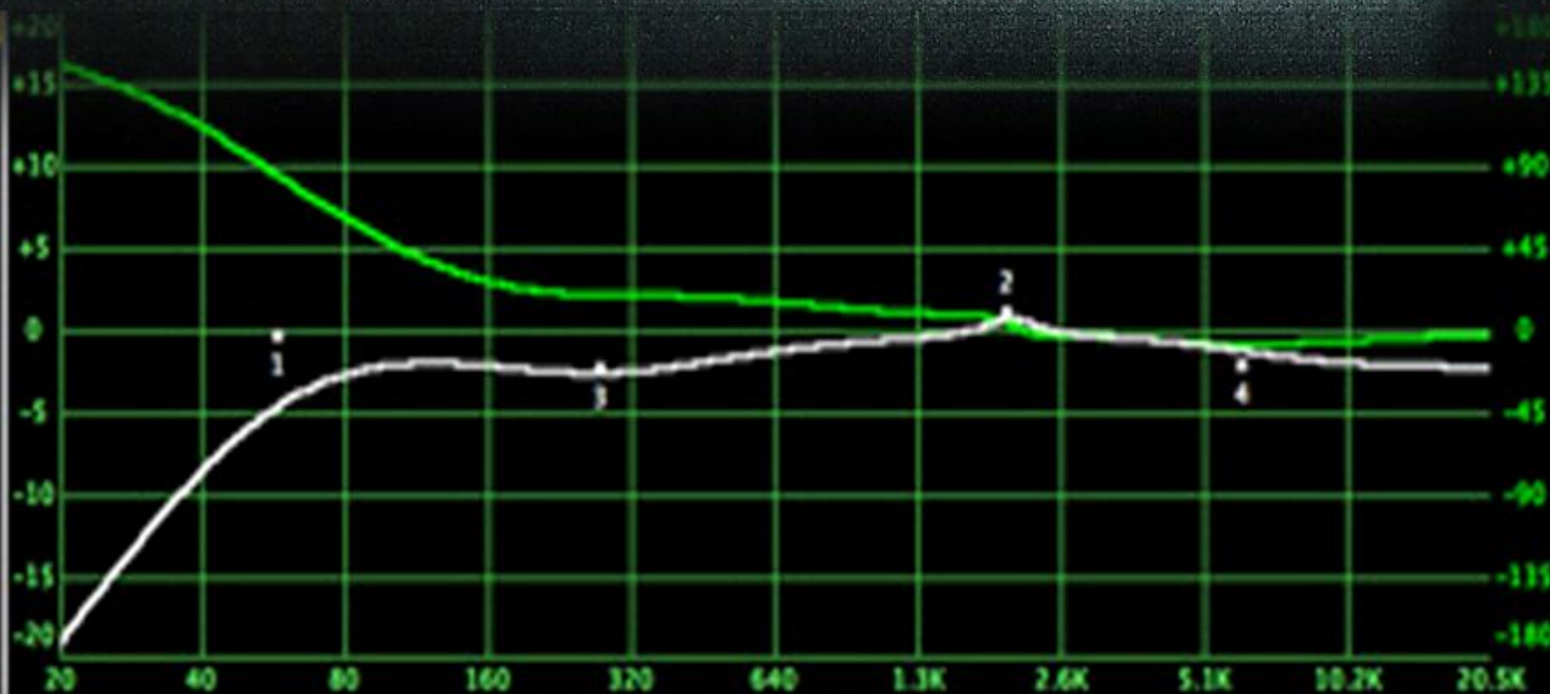


Signal Processing: An International Journal (SPIJ)

ISSN : 1985-2339

VOLUME 3, ISSUE 4

PUBLICATION FREQUENCY: 6 ISSUES PER YEAR



Editor in Chief Dr Saif alZahir

Signal Processing: An International Journal (SPIJ)

Book: 2009 Volume 3, Issue 4

Publishing Date: 31 - 08 - 2009

Proceedings

ISSN (Online): 1985 - 2339

This work is subjected to copyright. All rights are reserved whether the whole or part of the material is concerned, specifically the rights of translation, reprinting, re-use of illustrations, recitation, broadcasting, reproduction on microfilms or in any other way, and storage in data banks. Duplication of this publication of parts thereof is permitted only under the provision of the copyright law 1965, in its current version, and permission of use must always be obtained from CSC Publishers. Violations are liable to prosecution under the copyright law.

SPIJ Journal is a part of CSC Publishers

<http://www.cscjournals.org>

©SPIJ Journal

Published in Malaysia

Typesetting: Camera-ready by author, data conversion by CSC Publishing Services – CSC Journals, Malaysia

CSC Publishers

Table of Contents

Volume 3, Issue 4, August 2009.

Pages

- 34 - 41 A New Approach for Speech Enhancement Based On Eigenvalue Spectral Subtraction
Jamal Ghasemi, Mohammad Reze Karami Mollaei.
- 42 - 54 Usefulness of Speech Coding in Voice Banking
M Satya Sai Ram, P. Siddaiah, M. Madhavi Latha.
- 55 – 63 Application Of Extreme Value Theory To Bursts Prediction
Abdelmahamoud Youssouf Dahab, Abas bin Md Said, Halabi bin.
- 64 - 72 Ofdm-cpm Ber Performance and FOBP Under IEEE802.16 Scenario
Alimohammad Montazeri.
- 73 - 82 Investigating the Effect of Mutual Coupling on SVD Based Beamforming over MIMO Channels
Feng Wang, Marek E. Bialkowski Xia Liu.

A New Approach for Speech Enhancement Based On Eigenvalue Spectral Subtraction

Jamal Ghasemi

*Faculty of Electrical and Computer Engineering,
Signal Processing Laboratory
Babol Noshirvani University of Technology
Babol, P.O. Box 47135-484, IRAN*

jghasemi@stu.nit.ac.ir

Mohammad Reza Karami Mollaei

*Faculty of Electrical and Computer Engineering,
Babol Noshirvani University of Technology
Babol, P.O. Box 47135-484, IRAN*

mkarami@nit.ac.ir

Abstract

In this paper, a phase space reconstruction-based method is proposed for speech enhancement. The method embeds the noisy signal into a high dimensional reconstructed phase space and uses Spectral Subtraction idea. The advantages of the proposed method are fast performance, high SNR and good MOS. In order to evaluate the proposed method, ten signals of TIMIT database mixed with the white additive Gaussian noise and then the method was implemented. The efficiency of the proposed method was evaluated by using qualitative and quantitative criteria.

Keywords: Eigenvalues, singular values decomposition, Spectral Subtraction, Speech enhancement.

1. INTRODUCTION

Speech enhancement aims to improve the performance of speech communication systems in noisy environments. Speech enhancement may be applied, for example, to a mobile radio communication system, a speech to text system, a speech recognition system, a set of low quality recordings, or to improve the performance of aids for the hearing impaired [6, 16 17]. Existing approaches to this task include traditional methods such as spectral subtraction [1, 16], Wiener filtering [16, 17], and Ephraim Malah filtering [2]. Wavelet-based techniques using coefficient thresholding approaches have also been applied for speech enhancement [3, 4, 13]. As alternative to these traditional techniques is studying speech as a nonlinear dynamical system [9, 10]. In [15] two nonlinear methods for speech enhancement based on Singular Value Decomposition are studied. In [11] chaoslike features have been proposed for speech enhancement. Generally, the approaches can be classified into two major categories of single-channel and multi-channel methods. Single channel speech enhancement is a more difficult task than multiple channel enhancements, since there is no independent source of information with which to help separating the speech and noise signals. In these applications, the spectral subtraction is one of the most popular methods in which noise is usually estimated during speech pauses [1, 7, 8, 14] In this research, a new speech enhancement method is presented by using Singular Value Decomposition (SVD) regarding to spectral subtraction idea. The efficiency of the proposed method is evaluated by using the qualitative and quantitative criteria. The organization of this paper is as follows: In Section 2, Spectral Subtraction (SS) method, phase space

reconstruction and Singular Value Decomposition (SVD) are discussed. In Section 3 and 4, suggested Eigenvalues Spectral Subtraction (ESS) algorithm and simulation results are presented respectively. Finally the paper will be concluded in section 5.

2. BACKGROUND

2.1 Spectral Subtraction Process

As a classic speech enhancement technique, Spectral subtraction (SS) works well when the noise is stationary. In this method noise spectra is estimated by using the silence segment and subtracted from the noisy signal spectra. For applying this method three conditions must be assumed [16]:

- a. Noise must be additive.
- b. Signal and noise must be uncorrelated.
- c. One canal must be accessible.

There are many methods that work based on Spectral Subtraction and the original of them is Power Spectral Subtraction (PSS).

- **Power Spectral Subtraction (PSS)**

Assuming the noise is additive, we can model the corrupted speech signal by following equation:

$$y(n) = s(n) + d(n) \quad (1)$$

Where $s(n)$ and $d(n)$ is clean speech signal and noise respectively. According to the second assumption, the signal and noise are uncorrelated, so we can write:

$$r_d(\eta) = D_0 \delta(\eta) \quad (2)$$

Where r_d is autocorrelation function of noise signal and D_0 is a constant [16]. According to the equation 2 and by supposing that $s(n)$ and $d(n)$ signals are stationary, we can show:

$$\Gamma_x(\omega) = \Gamma_s(\omega) + \Gamma_d(\omega) \quad (3)$$

Where Γ is the power spectral density (PSD). So, if we can estimate $\Gamma_d(\omega)$ we will be able to estimate $\Gamma_s(\omega)$ as equation 4.

$$\hat{\Gamma}_x(\omega) = \Gamma_s(\omega) + \hat{\Gamma}_d(\omega) \quad (4)$$

Noise is estimated from silence frames. PSD is related to Discrete-Time Fourier transform (DFT) as:

$$\Gamma_y(\omega) = \frac{Y(\omega)Y^*(\omega)}{N^2} = \frac{|Y(\omega)|^2}{N^2} \quad (5)$$

We can conclude from equation 4 and 5.

$$\left| \hat{S}(\omega) \right|^2 = |Y(\omega)|^2 - \left| \hat{D}(\omega) \right|^2 \quad (6)$$

As mentioned above when $s(n)$ and $d(n)$ are stationary, equation 3 and 4 will be correct. Since the clean speech signals are locally stationary in short-time frames and also the assumption that noise is stationary is more acceptable in short time intervals, windowing is applied to the corrupted speech signal. Then the spectral subtraction is applied to each frame. To estimate the speech signal frames, the other necessary factor is $\varphi_s(\omega)$ as the estimated phase spectrum of speech frame. Boll has shown [1] that in practical applications, it is sufficient to use the noisy phase spectrum as an estimation of clean speech phase spectrum.

$$\hat{\varphi}_s(\omega) = \varphi_y(\omega) \tag{7}$$

Therefore from equation 6 and 7, we can obtain the estimated speech frames as shown in equation 8.

$$\hat{S}(\omega) = \left| \hat{S}(\omega) \right| e^{j \hat{\varphi}_s(\omega)} = \left[\left| Y(\omega) \right|^2 - \left| \hat{D}(\omega) \right|^2 \right]^{1/2} e^{j \varphi_y(\omega)} \tag{8}$$

The PSS algorithm is shown in Fig. 1.

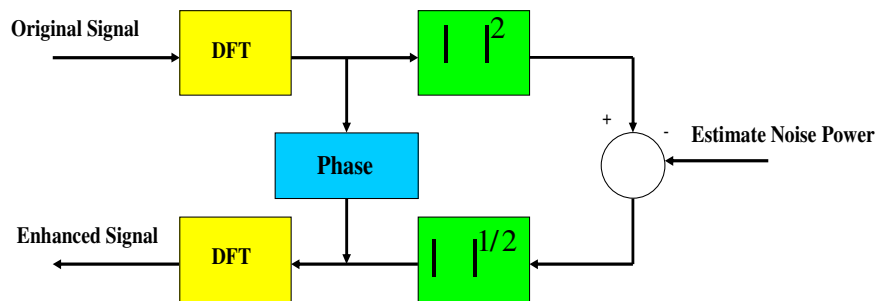


Figure 1. Spectral Subtraction Method

2.2 Phase Space Reconstruction

The dynamics of a system can be studied in a phase space, also called state space. Nonlinear time series methods perform analysis and processing in a reconstructed phase space, a time domain vector space whose dimensions are time lagged versions of the original time series [18, 19]. Takens time-delay-embedding method is probably the most common attractor reconstruction method in the literature [20]. Takens showed that if the embedding dimension is large enough, the reconstructed phase spaces have been shown to be topologically equivalent to the original system. Specifically, a scalar time series can be disclose in a multidimensional phase space using time delay coordinates. A brief describe of The Takens's method is as follows:

Given the time series $\{s_n, n = 1, 2, \dots, N\}$, the reconstructed attractor consists of the m vector

$$S_n = (s_n, s_{n+\tau}, s_{n+2\tau}, \dots, s_{n+(m-1)\tau}) \tag{9}$$

Where τ and m are the time delay and embedding dimension respectively. A reconstructed phase space matrix S of dimension m and lag τ is called a trajectory matrix and defined by:

$$S = \begin{bmatrix} S_1 \\ S_2 \\ \vdots \\ S_M \end{bmatrix} = \begin{bmatrix} s_1 & s_{1+\tau} & \cdots & s_{1+(m-1)\tau} \\ s_2 & s_{2+\tau} & \cdots & s_{2+(m-1)\tau} \\ \vdots & \vdots & \ddots & \vdots \\ s_M & s_{M+\tau} & \cdots & s_{M+(m-1)\tau} \end{bmatrix} \quad (10)$$

Where in each row S_i , $i = 1, 2, \dots, M$ represent individual points in the reconstructed phase space. The number of the points is $N = M + (m - 1)\tau$.

2.3 Singular Value Decomposition (SVD)

Singular Value Decomposition (SVD) is a very important tool in the problems of digital signal processing and data statistical analysis. The aim of SVD is to reduce the dimensions of a dataset as the reduced dataset still contains the variability features presented in the original data. The SVD theorem states that every real $m \times n$ ($m > n$) matrix X can be decomposed into a product of three matrices, as:

$$X = U \Sigma V^T \quad (11)$$

Where $U \in R^{m \times m}$ and $V \in R^{n \times n}$ are orthogonal matrices, i.e. $U^T U = I \in R^{m \times m}$ and $V^T V = I \in R^{n \times n}$ (with I identity matrix) and

$$\Sigma = \begin{bmatrix} \sigma_1 & 0 & \cdots & 0 \\ 0 & \sigma_2 & \cdots & 0 \\ \vdots & \vdots & \ddots & \vdots \\ 0 & 0 & \cdots & \sigma_m \end{bmatrix} \quad (12)$$

Σ is a diagonal matrix with singular values $\sigma_1 > \sigma_2 > \dots > \sigma_m > 0$. The singular values are the non-negative square roots of the eigenvalues of the covariance matrix $X^T X$ [5].

3. SUGGESTED ALGORITHM: ESS METHOD

Since noise is a random phenomenon, if we build a trajectory matrix from a noise segment and apply SVD on it, related σ_i s steadily reduce. Comparing the clean and noisy signals shows that the eigenvalues corresponding to the noisy signals are some different from the clean signals. This difference depends on noise amount added to clean signal and also is related to eigenvalues corresponding to the added noise. The eigenvalues contain some information about the signal energy so it is reasonable to perform a spectral analysis. According to the above discussion similar to SS algorithm, our proposed algorithm called ESS is shown in Fig. 2.

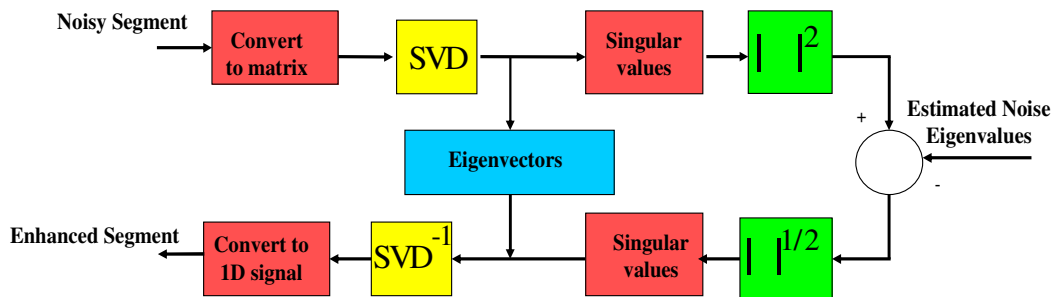


Fig.2: Eigenvalue Spectral Subtraction

In ESS, initial silence is used to estimate eigenvalues of the noise. The signal is segmented according to the silence segment and each segment is transformed to a matrix and SVD is applied (see section 2.2 and 2.3). As shown in Fig.2 the eigenvalues of the estimated noise are subtracted from eigenvalues of the noisy signal. The new obtained eigenvalues are used to reconstruct the corresponding segment. Simulation shows that, it is sufficient to use the noisy eigenvectors as an estimation of clean speech eigenvectors in each segment. It is noticeable that the eigenvectors are also saved to reconstruct the enhanced signal. The estimation and segmentation are shown in Fig. 3.

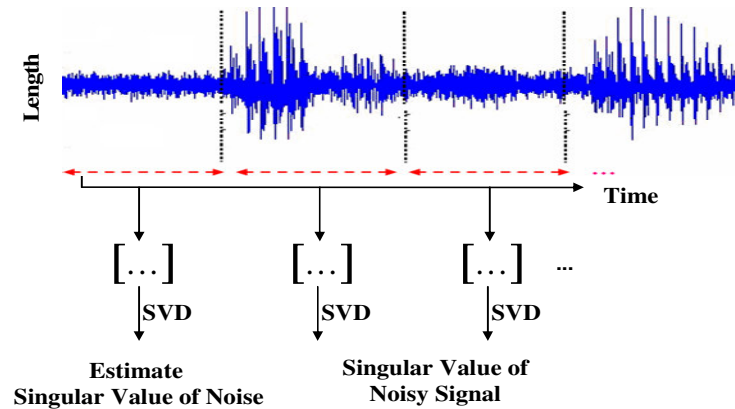


Fig. 3. Signal segmentation

4. SIMULATION RESULTS

Ten signals of TIMIT set were used to evaluate the algorithm efficiency. These signals are contaminated with additive white Gaussian noise. The new techniques were applied ten times to ten signals and the corresponding results were averaged. We arranged the simulation results as qualitative and quantitative results.

4.1 Quantitative Results

The signal to noise ratio (SNR) was used as quantitative criterion. Fig. 4 shows our algorithm results in comparison with results obtained by using the wavelet based method discussed in [4].

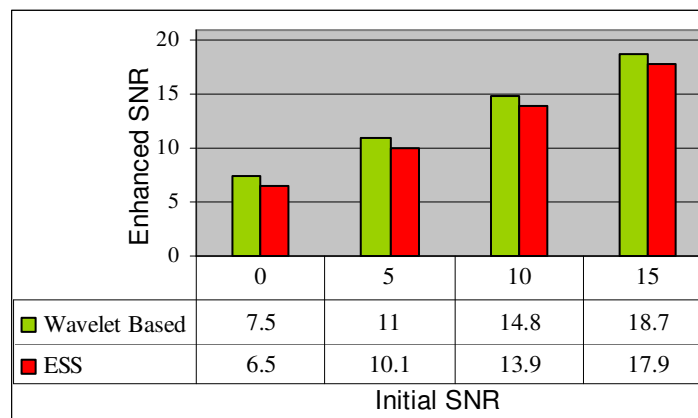


Fig 4. The comparison of the proposed method with wavelet based method

According to fig. 4 it is obvious that both algorithms perform much similarly to each other in aspect of SNR. It is noticeable that, since the proposed algorithm works in time domain, it is much faster than the last one which works in frequency domain (both algorithms implemented in Intel(R) Core(TM) 2Duo CPU).

4.2 Qualitative Results

For qualitative evaluation, we have shown the temporal results of clean, noisy and enhanced speech signal in Fig. 5.

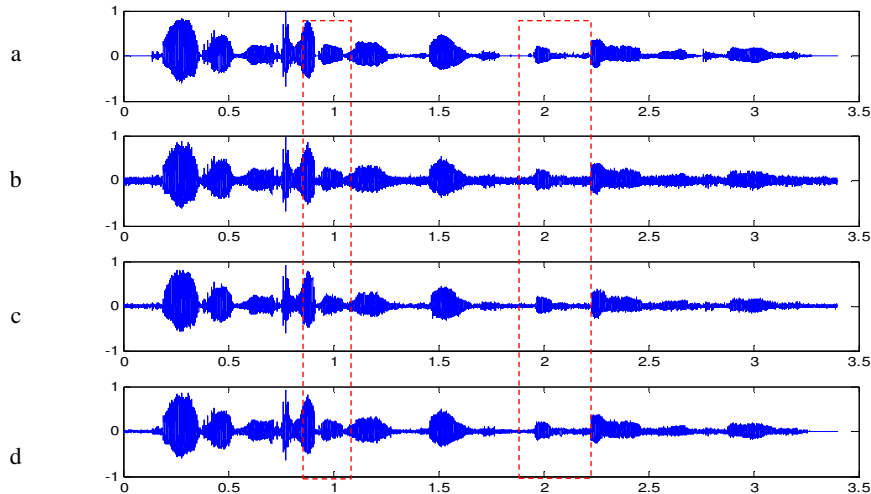


Figure 5: signals in time domain (ms)

- a: Clean signal
- b: Noisy signal
- c: Wavelet based enhancement
- d: ESS based enhancement

In Fig. 5, for simple comparison, two parts of the signals have been specified by using dashed lines. The signal enhanced by ESS (Fig. 5.d) is more similar to clean signal (Fig. 5.a) in comparison with wavelet-based enhanced signal (Fig. 5.c). For more investigation, audio experiments and the result of its implementation are presented.

- **Audio Experiment**

In this experiment, 6 persons (three women and three men) gave a mark to signals from 1 to 5. Ten speech signals with various SNRs (0, 5, 10 dB) and also their enhanced signals were used [12]. The mean opinion scores (MOS) corresponding ESS and wavelet-based method are illustrated in Fig. 6.

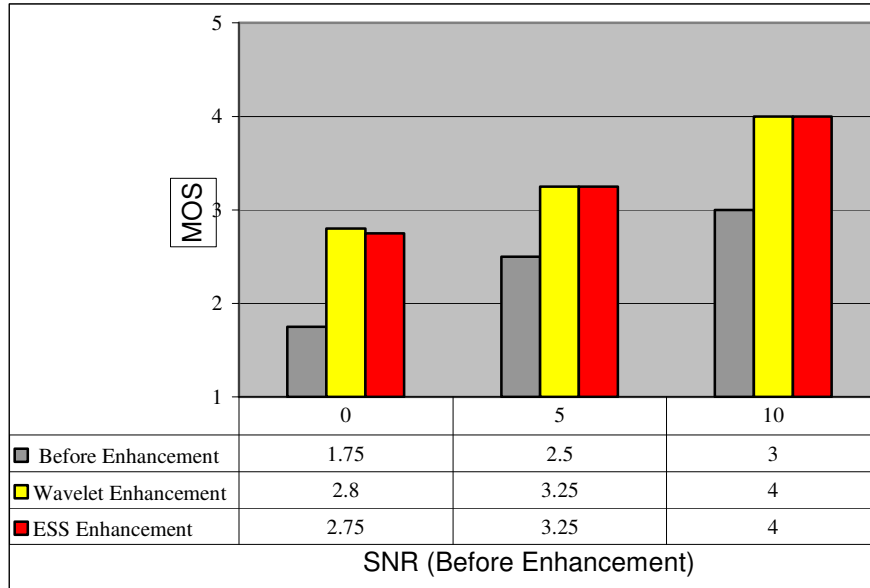


Fig. 6 MOS results for audio experiment

The MOS results show that both ESS and wavelet-based method have similar performance. So the hearing system of human beings is intelligence, it may neglect the noise undesirable and as a result, the audio test in both methods lead to the same results.

5. CONCLUSION

In this paper a new method (ESS) for speech enhancement was proposed. ESS is evaluated by using various criteria of quality and quantity. By using the mentioned criteria, it is presented that this method can compete with other speech enhancement methods. As seen in Fig.4 and 5 the proposed method provides proper performance in comparison with wavelet based method in terms of SNR. Mean opinion score also verifies the efficiency of the proposed method. Since ESS works in time domain it has faster than the frequency based methods. Another advantage of the proposed algorithm is that it does not require any voiced/unvoiced detection process by which the performance of the system is highly decreased. All of these mentioned advantages make ESS suitable for real time applications.

6. REFERENCES

1. S.F. Boll, "Suppression of acoustic noise in speech using spectral subtraction". IEEE Transactions Acoustics Speech Signal Process. 27, 113:120, 1979.
2. Y. Ephraim, D. Malah, "Speech enhancement using a minimum mean-square error short-time spectral amplitude estimator". IEEE Transactions Acoust. Speech Signal Process. ASSP. 32 (6), 1109:1121. 1984.
3. D.L. Donoho, "Denoising by soft thresholding". IEEE Transactions Information Theory, 41(3), 613:627, 1995.
4. Y. Ghanbari, M. R. Karami-M, "A new approach for speech enhancement based on the adaptive thresholding of the wavelet packets", Speech Communication 48, 927:940, 2006
5. S. Sayeed, N. S. Kamel and R. Besar. "A Sensor-Based Approach for Dynamic Signature Verification using Data Glove". Signal Processing: An International Journal (SPIJ), 2(1):1:10,2008

6. O. O. Khalifa, Z. H. Ahmad, A-H A. Hashim and T. S. Gunawan "SMaTalk: Standard Malay Text to Speech Talk System". 2(5) 1:16, 2008
7. H. Gustafsson, S. E. Nordholm and I. Claesson, "Spectral Subtraction Using Reduced Delay Convolution and Adaptive Averaging". IEEE Transactions on Speech and Audio Processing, 9(8),799:807, 2001.
8. D. E. Tsoukalas, J. N. Mourjopoulos and G. Kokkinakis, "Speech Enhancement Based on Audible Noise Suppression". IEEE Transactions on Speech and Audio Processing, 5(6), 497:514, 1997.
9. M. Banbrook, S. McLaughlin, and I. Mann, "Speech characterization and synthesis by nonlinear methods", IEEE Transactions on Speech and Audio Processing, 7, 1:17, 1999
10. A. Kumar, S. K. Mullick, "Nonlinear Dynamical Analysis of Speech", Journal of the Acoustical society of America,100, 615:629, 1966.
11. R. Hegger, H. Kantz, and L. Matassini, "Denoising Human Speech Signals Using Chaoslike Features", Physical Review Letters, 84(14), 3197:31200, 2000.
12. H. Sameti, H. Sheichzadeh, Li Deng, R. L. Brennan, "HMM Based Strategies for Enhancement of Speech Signals Embedded in Nonstationary Noise", IEEE Transactions on Speech and Audio processing, 6(5), 1988.
13. D. Guo, W. Zhu, Z. Gao, J. Zhang, "A study of wavelet thresholding denoising". Paper presented at the International Conference on Signal Processing, Beijing, PR China,2000.
14. R. Martin, "Spectral Subtraction Based on Minimum Statistics". Paper presented at the Europe Signal Processing Conference, Edinburgh, Scotland, 1994
15. M. T. Johnson , A. C. Lindgren, R. J. Povinelli, X. Yuan, "Performance of Nonlinear Speech Enhancement Using Phase Space Recognition Struction", ICASSP 2003
16. J. R. Deller, J. H. L. Hansen, J. G. Proakis, "Discrete Time Processing of Speech Signals", second ed. IEEE Press, New York (2000)
17. S. Haykin. "Adaptive Filter Theory", third ed. Prentice Hall, Upper Saddle River, New Jersey (1996)
18. H. D. I. Abarbanel, "Analysis of Observed Chaotic Data". Springer, New York (1996)
19. H. Kantz, T. Schreiber, "Nonlinear Time Series Analysis", Cambridge University Press, Cambridge, England (1997)
20. F. Takens. "In Dynamical Systems and Turbulence", edited by D. A. Rand and L.-S. Young, Lecture Notes, in Mathematics Vol. 898, Springer-Verlag, New York (1981)

USEFULNESS OF SPEECH CODING IN VOICE BANKING

M. Satya Sai Ram

*Chalapathi Institute of Technology
Guntur, AP, INDIA*

m_satyasairam@yahoo.co.in

P. Siddaiah

*K.L.College of Engineering
Guntur, AP, INDIA*

siddaiah_p@yahoo.com

M. Madhavi Latha

*J.N.T.U College of Engineering
Hyderabad, A.P, INDIA*

mlmakkena@yahoo.com

Abstract

Voice banking is an excellent telephone banking service by which a user can access his account for any service at any time of a day, in a year. The speech techniques involved in voice banking are speech coding and speech recognition. This paper investigates the performance of a speech recognizer for a coded output at 20 bits/frame obtained by using various vector quantization techniques namely Split Vector Quantization, Multistage Vector Quantization, Split-Multistage Vector Quantization, Switched Split Vector Quantization using hard decision scheme, Switched Multistage Vector Quantization using soft decision scheme and Multi Switched Split Vector Quantization using hard decision scheme techniques. The speech recognition technique used for recognition of the coded speech signal is the Hidden Markov Model technique and the speech enhancement technique used for enhancing the coded speech signal is the Spectral Subtraction technique. The performance of vector quantization is measured in terms of spectral distortion in decibels, computational complexity in Kflops/frame, and memory requirements in floats. The performance of the speech recognizer for coded outputs at 20 bits/frame has been examined and it is found that the speech recognizer has better percentage probability of recognition for the coded output obtained using Multi Switched Split Vector Quantization using hard decision scheme. It is also found that the probability of recognition for various coding techniques has been varied from 80% to 100%.

Keywords: Voice banking, Product Code Vector Quantizers, Linear Predictive Coefficients, Line Spectral Frequencies.

1. INTRODUCTION

Among number of applications for Speech coding, one of its main application is its use in voice banking. Voice banking is an excellent telephone banking service, which makes the user to be in touch with his account information at any time of the day. Speech coding plays an important role in voice banking, which involves the recognition of the coded outputs from a telephone line for

performing a particular banking operation. The speech recognizer at the banking end tries to understand the compressed spoken words in some way or the other and will act thereafter.

This paper takes the advantage of voice banking application and examined the performance of a speech recognizer for the coded outputs obtained by using various vector quantization techniques at 20bits/frame. The vector quantization techniques used in this work are the Split Vector Quantization (SVQ) [1-2], Multistage Vector Quantization (MSVQ) [3], Split-Multistage Vector Quantization (S-MSVQ) [4], Switched Split Vector Quantization (SSVQ) using hard decision scheme[3], Switched Multistage Vector Quantization (SWMSVQ) using soft decision scheme [5] and Multi Switched Split Vector Quantization (MSSVQ) using hard decision scheme [6-7].

Voice Banking is very useful in daily life, an excellent telephone banking service that makes the user to have an access to his account information, and other banking services 24 hours a day, 7 days a week and 365 days a year, just by making a simple phone call. With voice banking the user can have an access to the following services:

- 1) The user can check for balances on all his current, savings, and loan accounts.
- 2) The user can know the history of his account like the recent deposits, debits, check payments and interests.
- 3) The user can make funds transfer between two accounts and can make loan payments.
- 4) The user can check for interest rates on deposits and on various types of loans.
- 5) The user can stop the payments to be made.
- 6) The user can make a report about the lost or stolen card.
- 7) The user can have information about the bank branches, ATM locations and working hours.
- 8) The user can speak to the banks customer service center at any time of the day.

various other services can also be provided to the customers depending on the bank.

The speech techniques involved in voice banking are the speech coding, speech enhancement and speech recognition. Speech coding is used to compress the words spoken by the user before transmitting them over a telephone line. The speech enhancement techniques are used to remove the noise content before and after compression prior to applying them to a speech recognizer at the banking end. The speech recognition technique is used to recognize the compressed words spoken by the user. The speech parameters used for coding are the Line Spectral Frequencies (LSF) [8-9], so as to ensure filter stability after quantization. The parameters that can be used for speech recognition are the Linear Predictive Coefficients (LPC) and Mel-Frequency Cepstral Coefficients (MFCCs). In this work the parameters used for recognition are the Linear Predictive Coefficients. To improve the performance of recognition Energy, Delta and Acceleration coefficients must be used, but in this paper they are not used because if they are used, the generation of codebooks becomes a difficult task as the number of samples per vector increases.

The speech recognition technique used for the recognition of the coded outputs is the Hidden Markov Model (HMM) technique [10-11]. HMM is a collection of various statistical modeling techniques, in which the transition probability matrix is estimated with the help of the Baum Welch algorithm [11], the emission matrix is generated by using the K-means clustering algorithm and is estimated using the Baum Welch algorithm. The Viterbi algorithm can also be used for the estimation of the transition and emission matrices. For a given sequence the most likely sequence path is estimated using the Viterbi algorithm [11], from which the probability of a particular sequence is estimated using the forward algorithm or the backward algorithm. The stages involved in voice banking are: 1) Top level dialogue structure 2) Login mode 3) Account Balance Sub-Dialogue 4) Funds Transfer Sub-Dialogue [12].

2. TOP LEVEL DIALOGUE STRUCTURE

The Flow chart of a Top level dialogue structure is shown in Figure 1. The Top level dialogue structure consists of the following steps:

- 1) In the first step the voice banking system asks for the account number and PIN. When the user enters a valid account number and PIN, the voice banking system says that the 'Login is successful' and allows the user to enter the voice banking system or else it says the 'Login is unsuccessful'.
- 2) In the second step the voice banking system asks the user to select the required operation. If the user asks for the account balance, the account balance sub dialogue will be processed, if the user asks for funds transfer the funds transfer sub dialogue will be processed.
- 3) After performing the required banking operation the voice banking system asks the user 'Would you like to do any further operation?' If the user says 'Yes' the operation will go to step 2, if the user says 'No' it will say thank you for calling to voice banking and the process will be terminated.

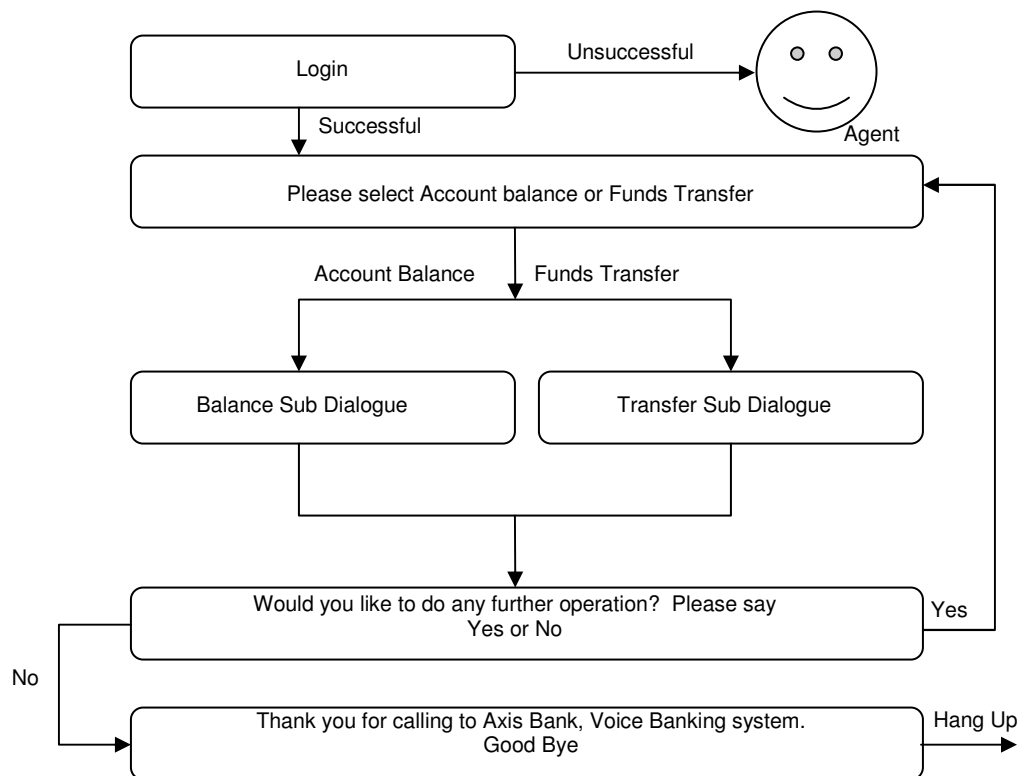


Figure 1: Top Level Dialogue Structure

3. LOGIN MODE

The Flow chart of the Login Mode in voice banking is shown in the Figure 3. The Login Mode consists of the following steps:

1. When a user dials for voice banking, a Welcome dialog appears and the voice banking system asks the customer to tell the account number.
2. When the customer tells the account number the voice banking system checks the account number for validation.
3. If the account number is valid, the voice banking system asks the customer to tell the PIN number, else it says that the account number is invalid and asks to try again. The account number given by the customer must be recognized by the voice banking system in three attempts otherwise the account will be blocked by the banking system.

- When the account number and PIN are valid the voice banking system allows the customer to perform the required transaction by saying that the 'Login is successful'.

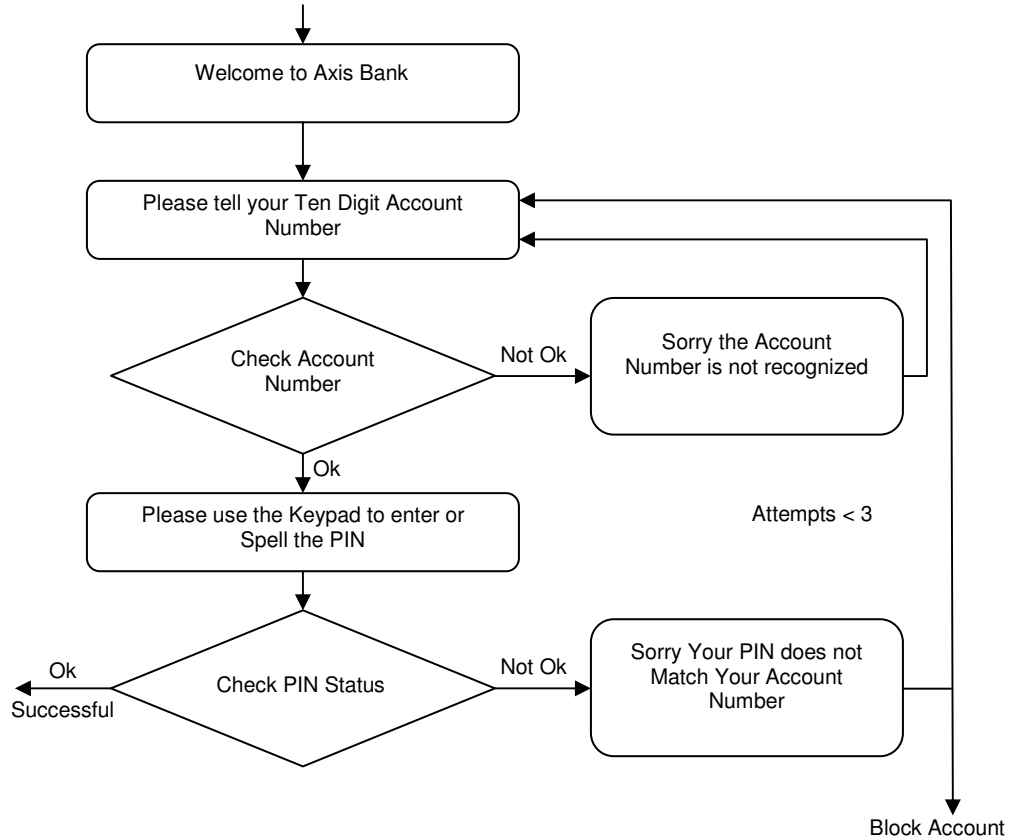


Figure 3: Login Mode

4. ACCOUNT BALANCE SUB-DIALOGUE

The Flow chart of the Account Balance sub-dialogue in voice banking is shown in the Figure 2.

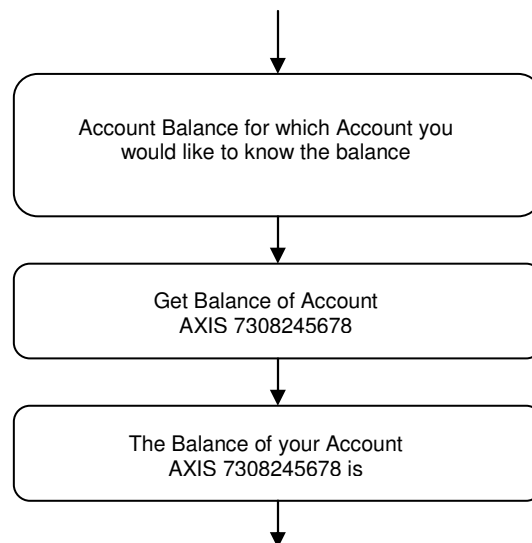


Figure 2: Account Balance sub-dialogue

The Account Balance sub-dialogue consists of the following steps:

1. When the user asks for account balance, the voice banking system asks for the type of account for which the user likes to know the balance.
2. When the user tells the type of account and account number, and if the account number is valid then the voice banking system will tell the balance of the account.

5. FUNDS TRANSFER SUB-DIALOGUE

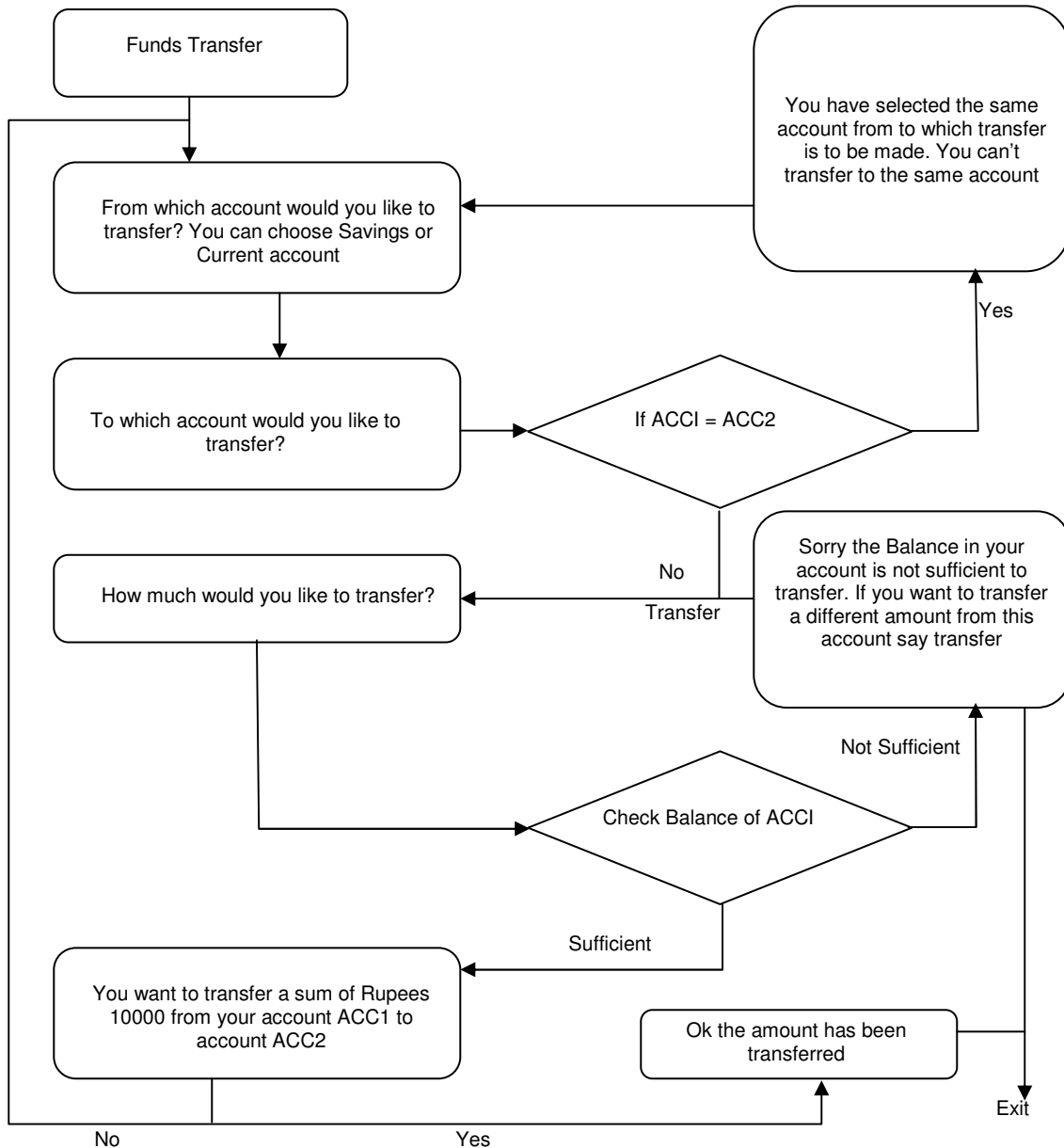


Figure 4: Funds Transfer sub-dialogue

The Flow chart of the Funds Transfer sub-dialogue in voice banking is shown in Figure 4. It consists of the following steps:

1. In the first step of funds transfer the voice banking system will ask the user from which account you would like to transfer, either savings or current account.
2. In the second step it asks for the account to which transfer is to be made.
3. In the third step when the user tells the account number, the voice banking system checks the account number to which transfer is to be made.
4. If both the account numbers to which transfer is to be made are same then the voice banking system says that you cannot transfer to the same account and the process will return back to step1.
5. If the two account numbers are not identical then the voice banking system asks 'How much would you like to transfer?'
6. In the fourth step when the user speaks for the amount to be transferred, the voice banking system checks the balance of the account from which transfer is to be made.
7. If the balance is not sufficient, the voice banking system says 'There is insufficient balance in the account' and asks to enter a different amount.
8. If the balance in the account is sufficient, the banking system says 'Do you want to transfer the amount from ACC1 to ACC2 ?' (Account1 to Account2).
9. When the user says 'Yes' the transfer will be made and if the user says 'No' it will return to step1.
10. When the transfer is made, the banking system says 'The transfer has been made' and the process will be terminated.

The compressed speech output must be of good quality, otherwise the speech recognizer may fail to recognize the spoken words, if it fails to recognize in three attempts the account will be blocked. So an efficient coding technique is required to compress the spoken words. In this work the performance of the speech recognizer has been observed for various coded outputs, obtained by using various vector quantization techniques at 20 bits/frame. The quantization techniques used for coding are SVQ, MSVQ, S-MSVQ, SSVQ using hard decision scheme, SWMSVQ using soft decision scheme, and MSSVQ using hard decision scheme techniques. The speech enhancement technique used is the 'Spectral subtraction' technique, it is used to remove the noise in the coded speech signal after transmission and the speech recognition technique used is the 'Hidden Markov Model technique'. The steps involved in speech coding, enhancement and recognition to obtain a good quality of speech for the voice bank recognizer are:

- 1) In the first step, the silence part of the speech signal must be removed by using the voice activation and detection technique.
- 2) In the second step, the speech signal must be coded using a vector quantization technique.
- 3) In the third step, the coded output with added channel noise must be enhanced by using an enhancement technique.
- 4) In the fourth step, the enhanced speech signal must be given as an input to the voice bank recognizer for recognizing.
- 5) Finally the probability of recognition can be computed as a measure of the recognition accuracy.

From results it has been observed that for the coded outputs obtained by using various vector quantization techniques and the recognition accuracy has been varied from 80% to 100%.

6. MULTI SWITCHED SPLIT VECTOR QUANTIZATION

The block diagram of a $p \times m \times sp$ Multi Switched Split Vector Quantizer is shown in Figure 5. In Figure 5, p corresponds to the number of stages, m corresponds to the number of switches, and sp corresponds to the number of splits. Each input vector 's' to be quantized, is applied to the first stage of a Multi Switched Split Vector Quantizer to obtain the quantized version of the input vector 's' given by $\hat{s}_1 = Q [s]$. The error vector at the first stage $e_1 = s - \hat{s}_1$ will be computed and is quantized using the Switched Split Vector Quantizer at the second stage to obtain the

quantized version of the error vector $\hat{e}_1 = Q[e_1]$. This process can be continued for the required number of stages. Finally the decoder takes the indices, I_i , from each stage and adds the quantized vectors at each stage to obtain the quantized version of the input vector \hat{s} given by $\hat{S} = Q[S] + Q[e_1] + \dots$, where $Q[S]$ is the quantized version of the input vector at the first stage, $Q[e_1]$ is the quantized version of the error vector at the second stage and so on [6-7].

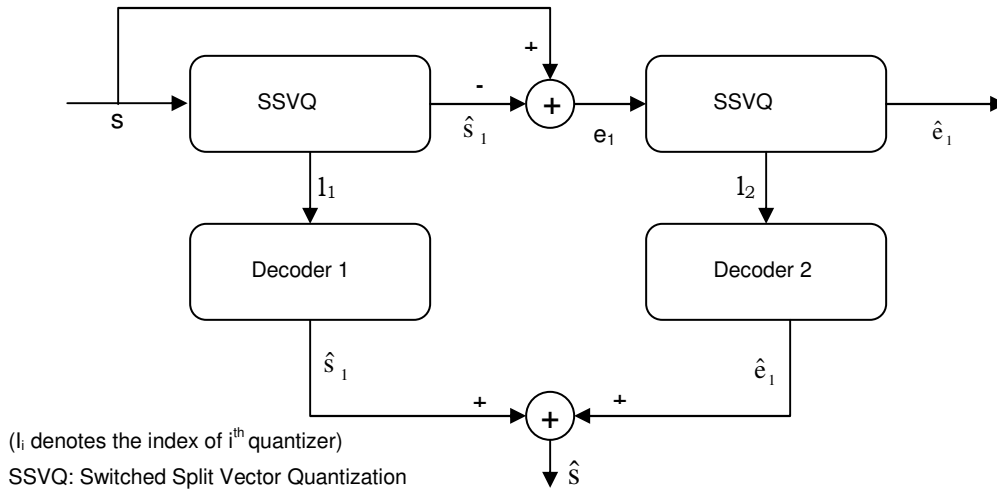


Figure 5: Block Diagram of MSSVQ

7. RESULTS

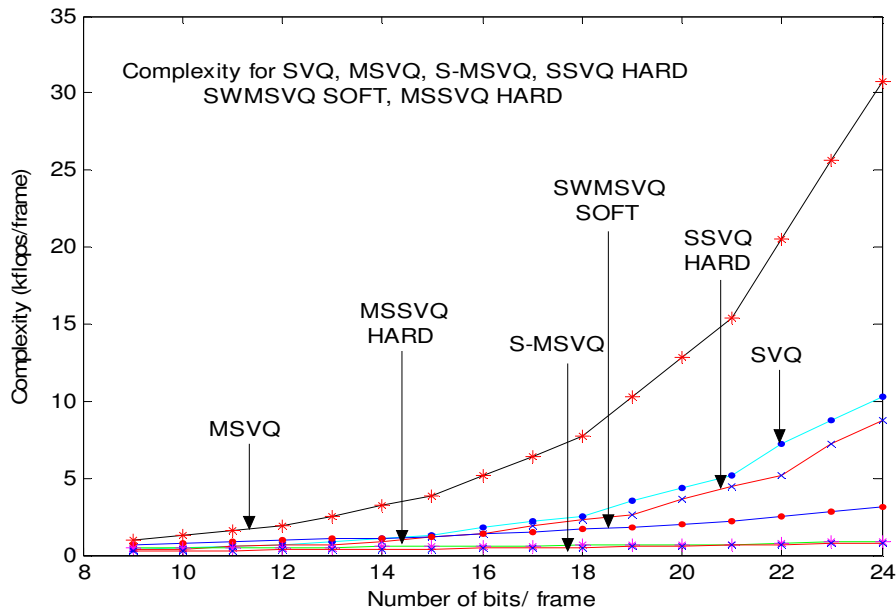


Figure 6: Complexity for SVQ, MSVQ, S-MSVQ, SSVQ hard, SWMSVQ soft, and MSSVQ hard

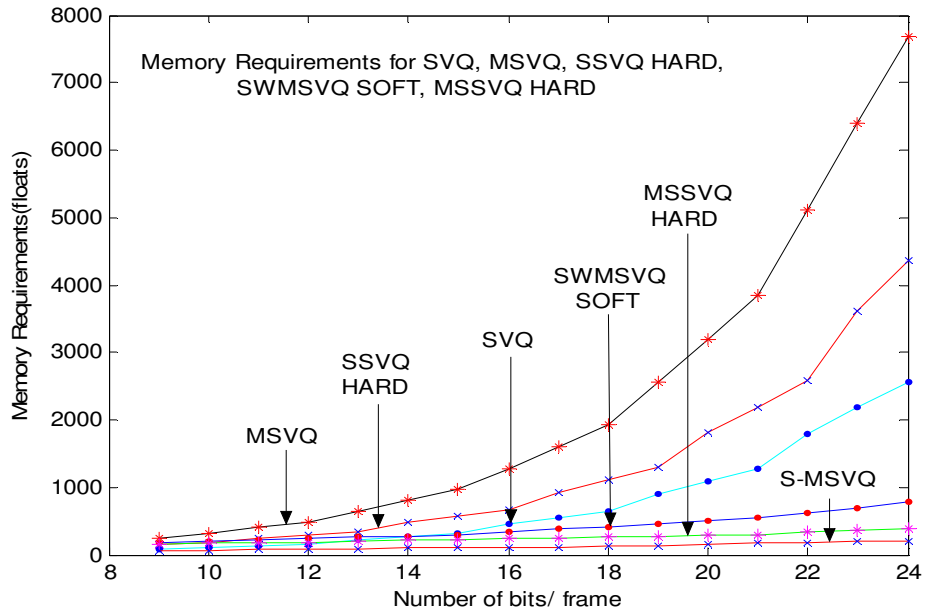


Figure 7: Memory requirements for SVQ, MSVQ, S-MSVQ, SSVQ hard, SWMSVQ soft, and MSSVQ hard

Table 1: Spectral distortion, Complexity, and Memory requirements for 3-part Split Vector Quantization

Bits / frame	SD (dB)	Percentage of outliers		Complexity (kflops / frame)	ROM (floats)
		2-4 dB	>4 dB		
24(8+8+8)	1.45	0.43	0	10.237	2560
23(7+8+8)	1.67	0.94	0	8.701	2176
22(7+7+8)	1.70	0.78	0.1	7.165	1792
21(7+7+7)	1.83	2.46	0.2	5.117	1280
20(6+7+7)	1.81	1.6	0.4	4.349	1088

Table 2: Spectral distortion, Complexity, and Memory requirements for 3-stage Multistage Vector Quantization

Bits / frame	SD (dB)	Percentage of outliers		Complexity (kflops / frame)	ROM (floats)
		2-4 dB	>4 dB		
24(8+8+8)	0.984	1.38	0	30.717	7680
23(8+8+7)	1.238	1.2	0.1	25.597	6400
22(8+7+7)	1.345	0.85	0.13	20.477	5120
21(7+7+7)	1.4	1.08	0.3	15.357	3840
20(7+7+6)	1.41	1.1	0.4	12.797	3200

Table 3: Spectral distortion, Complexity, and Memory requirements for 3-part, 3-stage Split-Multistage Vector Quantization

Bits / frame	SD (dB)	Percentage of outliers		Complexity (kflops / frame)	ROM (floats)
		2-4 dB	>4 dB		
24(8+8+8)	0.0345	0	0	0.807	204
23(8+8+7)	0.0385	0	0	0.759	192
22(8+7+7)	0.0378	0.1	0	0.711	180
21(7+7+7)	0.0382	0.2	0	0.663	168
20(7+7+6)	0.0389	0.3	0	0.599	0.152

Table 4: Spectral distortion, Complexity, and Memory requirements for 2- switch 3-part Switched Split Vector Quantization using hard decision scheme

Bits / frame	SD (dB)	Percentage of outliers		Complexity (kflops / frame)	ROM (floats)
		2-4 dB	>4 dB		
24(1+7+8+8)	0.957	1.06	0	8.78	4372
23(1+7+7+8)	1.113	1.29	0.14	7.244	3604
22(1+7+7+7)	1.119	0.52	1.3	5.196	2580
21(1+6+7+7)	1.127	1.3	0.56	4.428	2196
20(1+6+6+7)	1.09	1.3	0.63	3.66	1812

Table 5: Spectral distortion, Complexity, and Memory requirements for 3-stage 2-switch Switched Multistage Vector Quantization using soft decision scheme

Bits / frame	SD (dB)	Percentage of outliers		Complexity (kflops / frame)	ROM (floats)
		2-4 dB	>4 dB		
24(1+7+1+7+1+7)	0.91	0.56	0.81	3.111	780
23(1+7+1+7+1+6)	0.87	1.05	0.31	2.791	700
22(1+7+1+6+1+6)	1.1	1.45	0.63	2.471	620
21(1+6+1+6+1+6)	1.18	0.6	1.89	2.151	540
20(1+6+1+6+1+5)	1.15	0.69	1.83	1.99	500

Table 6: Spectral distortion, Complexity, and Memory requirements for 2-switch 3-part 3-stage Multi Switched Split Vector Quantization using hard decision scheme

Bits / frame	SD (dB)	Percentage of outliers		Complexity (kflops / frame)	ROM (floats)
		2-4 dB	>4 dB		
24(1+7+1+7+1+7)	0.0322	0	0	0.9	396
23(1+7+1+7+1+6)	0.0381	0	0	0.836	364
22(1+7+1+6+1+6)	0.0373	0	0	0.772	332
21(1+6+1+6+1+6)	0.0377	0	0	0.708	300
20(1+6+1+6+1+5)	0.0376	0	0	0.684	288

Table 7: Probability of recognizing a word ONE at 20 bits / frame by using SVQ, MSVQ, S-MSVQ, SSVQ using hard decision scheme, SWMSVQ using soft decision scheme and MSSVQ using hard decision scheme

NAME	PROBABILITY OF RECOGNITION					
	SVQ	MSVQ	S-MSVQ	SSVQ	SWMSVQ	MSSVQ
ZERO	-16.4401	-14.3510	-11.0312	-17.3314	-15.639	-10.3625
ONE	-19.6432	-16.8930	-19.3211	-20.8234	-21.3025	-19.1769
TWO	-19.6941	-16.9001	-14.6350	-15.0031	-15.918	-14.220
THREE	-16.3331	-13.1160	-12.0561	-17.5689	-17.493	-11.1311
FOUR	-15.9137	-15.6603	-17.3426	-17.7058	-16.749	-16.9621
FIVE	-17.0071	-17.0531	-17.1076	-19.1743	-17.069	-16.5635
SIX	-18.0012	-14.5134	-14.1384	-18.9013	-18.938	-13.3014
SEVEN	-15.9981	-13.0007	-13.4420	-15.1007	-19.687	-11.6120
EIGHT	-14.8371	-14.5563	-13.8603	-15.2330	-11.806	-12.1421
NINE	-19.6801	-17.1281	-20.1107	-21.1163	-20.031	-19.106
TEN	-18.9561	-15.0081	-18.3214	-18.4418	-13.671	-17.5038
YES	-16.8341	-14.3842	-17.2014	-17.3341	-20.398	-16.6141
NO	-20.3259	-14.9802	-18.6345	-21.9276	-16.943	-18.0170
SUCCESSFULL	-13.9253	-10.3310	-11.1010	-14.0140	-10.621	-9.6210
UNSUCCESSFULL	-13.1109	-10.5676	-11.0048	-15.0121	-11.006	-9.7128
% RECOGNITION	80.00%	80.00%	93.33%	86.66%	100%	100%

The computational complexity, and memory requirements of MSSVQ using hard decision scheme is less when compared to all the product code vector quantization techniques except for S-MSVQ which can be observed from Tables 1-6 and from Figure's 6 and 7. Table 7 shows the probability of recognizing a particular coded word 'ONE' obtained by using SVQ, MSVQ, S-MSVQ, SSVQ using hard decision scheme, SWMSVQ using soft decision scheme and MSSVQ using hard decision scheme at 20 bits/ frame. The reason for choosing 20 bits/frame is that with MSSVQ using hard decision scheme the transparency in quantization has been achieved at 20 bits/frame, so 20 bits/frame is taken as the reference. From Table 7 it can be observed that for the utterance 'ONE' as an input the probability of recognition is better for SWMSVQ using soft decision scheme and MSSVQ using hard decision scheme and it is 100%. But it is advantageous to use MSSVQ using hard decision scheme for voice banking application as its spectral distortion is less when compared to all the product code vector quantization techniques which can be observed from tables 1 to 6. So it is proved that MSSVQ using hard decision scheme can be better used in voice banking applications for coding of the speech signals.

8. CONCLUSION

The Speech recognizer using HMM performs well for the coded output obtained by using MSSVQ using hard decision scheme at 20 bits / frame, as it has less spectral distortion. MSSVQ can have better marketability as it has less computational complexity and memory requirements. From results it is observed that the probability of recognition has been varied from 80% to 100% for various vector quantization techniques and for Switched Multistage Vector Quantization using soft decision scheme and Multi Switched Split Vector Quantization using hard decision scheme the probability of recognition is 100%. But it is proved that Multi Switched Split Vector Quantization technique using hard decision scheme is superior in terms of spectral distortion, computational complexity and memory requirements when compared to other product code vector quantization techniques. So Multi Switched Split Vector Quantization using hard decision scheme is proved to be better and is having performance closer to Split-Multistage Vector Quantization technique. So Multi Switched Split Vector Quantization using hard decision scheme is proved to be the better coding technique for voice banking application. The performance can be further improved by increasing the number of training vectors, bits used for codebook generation, the number of states of an utterance, by using an efficient algorithm for the generation of emission matrix that takes into account the entire training set unless the K-means clustering that randomly picks vectors from the training set for the generation of an emission matrix, and by using a software having greater degree of precision. With 'Matlab' the generation of an emission matrix with k-means is difficult when the number of states is more for a particular utterance.

9. REFERENCES

1. Paliwal K.K, Atal, B.S. "Efficient vector quantization of LPC Parameters at 24 bits/frame". in: Proc.IEEE Int. Conf. Acoust, Speech, Signal Processing, (1): 661-664,1991.
2. Paliwal. K.K, Atal, B.S. "Efficient vector quantization of LPC Parameters at 24 bits/frame". IEEE Trans. Speech Audio Process, 1(1): 3-14, 1993.
3. Stephen, So., Paliwal, K. K. "Efficient product code vector quantization using switched split vector quantizer". Digital Signal Processing journal, Elsevier, 17(1): 138-171,2007.
4. Woo-Jin Han, Eun-Kyoung Kim, Yung-Hwan Oh. "Multi codebook Split Vector Quantization of LSF parameters". IEEE Trans. Signal Processing, 9: 418-421, 2002.
5. K.Srinivas, M.Madhavi Latha, P.Siddaiah, M.satya Sai Ram.(July 2008a). Switched Multi stage vector quantization using soft decision scheme. Proceedings of the 2008 International conference on Image processing, computer vision and pattern recognition (IPCV 2008), WORLD COMP2008, 2: 587-591, 2008.
6. M.Satya Sai Ram, P.Siddaiah, M.MadhaviLatha. "Multi Switched Split Vector Quantization of Narrow Band Speech Signals", Proceedings World Academy of Science, Engineering and Technology, WASET, 27: 236-239,2008.
7. M.Satya Sai Ram, P.Siddaiah, M.MadhaviLatha. "Multi Switched Split Vector Quantizer", International Journal of Computer, Information, and Systems science, and Engineering, IJCISSE, WASET, 2(1): 1- 6, 2008.
8. Kleijn, W.B. Tom Backstrom, Paavo Alku."On Line Spectral Frequencies". IEEE Signal Processing Letters, 10(3): 75-77, 2003.
9. Soong. F, Juang. B. "Line spectrum pair (LSP) and speech data compression", IEEE Conference. On Acoustics, Speech Signal Processing, 9(1): 37-40, 1984.
10. Rabiner Lawrence, Juang Bing-Hwang. "Fundamentals of speech Recognition". Prentice Hall, New Jersey, ISBN 0-13-015157-2, 1993.
11. Rabiner L.R. "A tutorial on Hidden Markov Models and selected applications in speech recognition". Poceedings of the IEEE, 77(2): 257-286, 1989.
12. Robert Dale. "Dialog Design Specification: A Voice Banking Application," Macquarie University - Sydney, 0.1: 1-22, 2002.

APPLICATION OF EXTREME VALUE THEORY TO BURSTS PREDICTION

Abdelmahamoud Youssouf Dahab

*Computer & Information Sciences Department,
Universiti Teknologi PETRONAS,
Bandar Seri Iskandar, Tronoh, 31750 Perak, Malaysia.*

dahab_tc@hotmail.com

Abas bin Md Said

*Computer & Information Sciences Department,
Universiti Teknologi PETRONAS,
Bandar Seri Iskandar, Tronoh, 31750 Perak, Malaysia*

abass@petronas.com.my

Halabi bin Hasbullah

*Computer & Information Sciences Department,
Universiti Teknologi PETRONAS,
Bandar Seri Iskandar, Tronoh, 31750 Perak, Malaysia.*

halabi@petronas.com.my

Abstract

Bursts and extreme events in quantities such as connection durations, file sizes, throughput, etc. may produce undesirable consequences in computer networks. Deterioration in the quality of service is a major consequence. Predicting these extreme events and burst is important. It helps in reserving the right resources for a better quality of service. We applied Extreme value theory (EVT) to predict bursts in network traffic. We took a deeper look into the application of EVT by using EVT based Exploratory Data Analysis. We found that traffic is naturally divided into two categories, Internal and external traffic. The internal traffic follows generalized extreme value (GEV) model with a negative shape parameter, which is also the same as Weibull distribution. The external traffic follows a GEV with positive shape parameter, which is Fréchet distribution. These findings are of great value to the quality of service in data networks, especially when included in service level agreement as traffic descriptor parameters.

Keywords: Traffic Bursts, Extreme Value Theory, Prediction, Quality of Service, Self-Similar.

1. INTRODUCTION

Extreme bursts have detrimental effects to network traffic and quality of service. These effects may go far beyond congestion and delay. The Quality of Service (QoS) suffers as well. To remedy, bursts need to be predicted in advance so that proper measures can be taken to mitigate their effect. We need to understand the structure of traffic correctly so that we will be able to predict bursts and enhance the QoS offered.

The discovery of the self-similarity of network traffic is a mile stone in computer networks. All the old method of modeling the traffic may not withstand the self-similarity of the network traffic. New models based on the self-similar properties are being developed [8, 15]. Self-similarity means that traffic is bursty over wide range of scales. Bursts can be defined as high aggregation of data in a relatively very small time interval. This definition is a general one and can be defined more precisely depending on the given contexts.

Traffic prediction problem has been approached using different techniques. These techniques range between stochastic processes based methods [10, 11], Autoregressive moving average (ARMA) with its variants FARIMA, ARIMA to Artificial Neural Network (ANN) and Wavelet Based predictors, recent survey of these methods with references is given in [6]. However, these techniques are using the whole set of data and can be computationally expensive. We suggest the Extreme Value Theory (EVT) as a framework to deal with the bursts prediction problem.

EVT is a branch of knowledge that stems out of statistics. It is analogous to the central limit theorem (CLT). While the CLT deals with the distribution of the sample mean and tells us that it converges asymptotically to a normal distribution, the EVT deals with sample maximum and tells that it converges asymptotically to one of three distributions (Gumbel, Weibull, and Fréchet), these distribution limits are combined in a single representation called Generalized Extreme Value Distribution (GEV). EVT is a rational framework to the problem of burst prediction. It needs only a subset of the data to work on. This will greatly reduce the time space-complexity of the method. Another advantage is that the EVT is being developed for these kinds of problems, i.e. predicting extreme events based on subset of the data. It has been in use in diverse fields such as Insurance, Finance, and Hydrology etc, see [2, 5].

Recent studies suggested EVT as a framework for modeling different types of traffic [4, 12, 18, 19]. In [19], Masato Uchida used the throughput as a network parameter to be modeled. He argued that throughput, link usage rate, packet loss rate and delay time can be used to predict telecommunication quality. He used the Peak Over Threshold (POT) method for the modeling and fitted a generalized Pareto distribution. He showed that the POT using GPD is better in approximating the unknown part of the data than the previously commonly used lognormal distribution.

In [12], authors also used POT method for the analysis of wireless traffic. They fitted a GPD model and compared their model to the lognormal, Gamma, Exponential models. The computational overhead is clearly reduced when using the EVT model because we need only a subset of the data to work on.

However, these studies are far from complete. They did not include a rigorous check to see the applicability of the EVT analysis. They applied the theory of EVT and in particular the POT method with the assumptions that it holds true. They did not include any preliminary analysis of the data to check whether the theory assumptions hold or not. Such steps are important and crucial for the success of the model. One of the reasons for this is that dependent correlated data do not necessarily converge to the classical form of the three distributions limits. As shown in [9], if the data are highly dependent, then a further parameter called extremal index needs to be carefully introduced.

In a previous work, we applied the EVT to the internal traffic [4]. In this work, we extend our model to the external traffic as well. We applied EVT more faithfully by using EVT based exploratory tools. Our findings are unique. We found that traffic distinguishes itself into external and internal by assuming different signs in GEV model. Using the Block Maxima (BM) method, the external traffic follows a GEV with positive shape parameter, which is analogous to the traffic bursts following extreme Fréchet distribution. Internal traffic follows a GEV with a negative shape parameter. This also means that traffic bursts follow extreme Weibull distribution.

The structure of this paper is as follows. First, we present EVT based model selection tools. We apply them to Belcore traffic traces. We then estimate the parameters and show our prediction

Dataset	Type	Size	Source	Parameters
BC-pAug98	Internal Traffic	31429	Belcore	
BC-pOct98	Internal Traffic	15795		
BC-Oct89Ext	External Traffic	759431		
FGN078	Internal Traffic	10000	Simulated FGN	H=0.78
LFSN	External Traffic	10000	Simulated LFSN	H=0.75, Alpha=1.5

results, and then we conclude.

TABLE 1 : Datasets

2. MODEL SELECTION TOOLS

Visualizing data is a very important step before a serious decision is to be taken about the underlying process. A great deal of work has been done to illustrate this point. Such analysis bears the name of Exploratory Data Analysis (EDA). In our work, we refer to EDA as EVT based model selection tools. Selecting the right model is important. In this section, we discuss some of EVT based model selection tools. Namely, Records, Maximum to Sum Ratio, Gumbel Plot, Mean Excess plot. Other tools such as QQ-plot and Hill plot will be discussed here. Using these tools, we analyze the Ethernet traffic traces from Belcore data and simulated ones.

Our five data sets consist of three data sets from Belcore Labs [21] and the other two are simulated traces for both internal and external traffic [1, 14, 17]. We transformed Belcore traces into bitrate per 0.1 second using simple MATLAB routines. The simulation of the internal trace is based on Fractional Gaussian Noise (FGN) model suggested by Norros in [14] and the simulated trace of the external traffic is based on Linear Fractional Alpha Stable Noise (LFSN) model, see [20]. A summary of the data under study is given in Table1.

2.1 Records

Records can be used as exploratory tool in distinguishing between i.i.d and non i.i.d data. The number of records of i.i.d data grows very slowly [5]. This fact allows us to use records in our traffic data and check it against expected records in a typically known i.i.d data. If there is a match in the number of records, then we may say that our data can be modeled as i.i.d otherwise we say that our traffic data cannot be modeled as coming from i.i.d random process.

A record occurs if $X_n > M_{n-1} = \max(X_1, \dots, X_{n-1})$. By definition X_1 is a record. Let I be indicator function, the record counting process N is given by

$$N_1 = 1, N_n = 1 + \sum_{k=2}^n I_{X_k > M_{k-1}}, n \geq 2$$

How would Records help? To answer this question, we tabulated the number of expected records in a typical i.i.d dataset [5]. For the purpose of comparison, we computed the number of records in the examined datasets.

A dramatic departure from the expected values in this table suggests clearly rejecting i.i.d assumption. From Table 2, it is clear that disparity exists between the number of records in our data and those expected from a typical i.i.d dataset. For the Aug98 data, it assumes higher values than the average, while the Oct98 data assumes below average values. Nevertheless, they are still within one standard deviation from the mean. So the i.i.d. assumption is a valid one.

$n = 10^k$	EN	\sqrt{VN}	BC-pAug98	BC-pOct98	FGN078	LFSN	Oct89Ext
1	2.9	1.2	2	3	1	4	1

2	5.2	1.9	7	4	2	6	2
3	7.5	2.4	10	7	7	9	6
4	9.8	2.8	12	11	7	12	12

E 2: Records

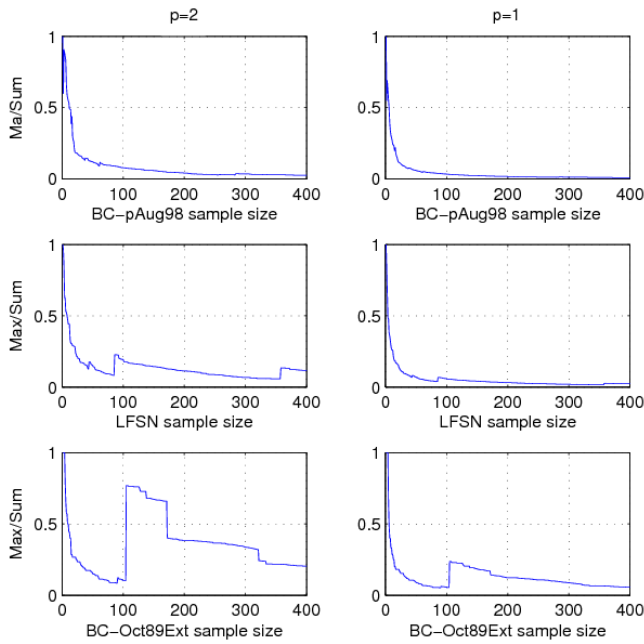


Fig. 1. Maximum to Sum Ratio with $p=2$, and $p=1$ for bytes/100 ms datasets.

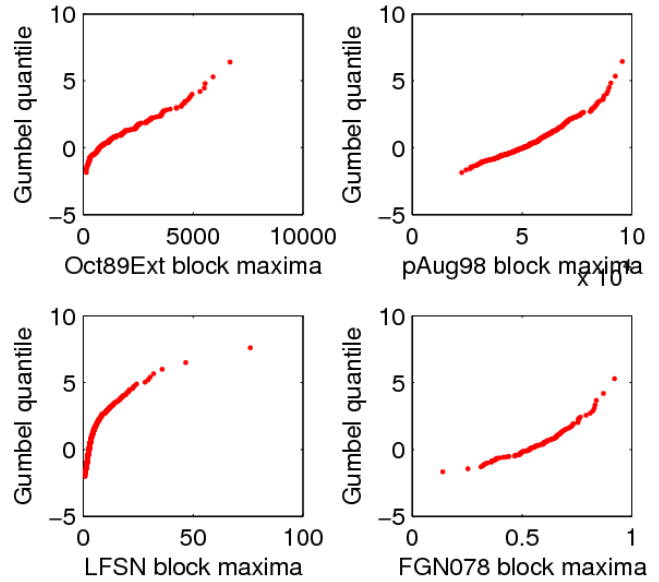


Fig.2. Gumbel plots. Some plots show concave departure from linearity and some show a convex departure from linearity.

2.2 Maximum to Sum Ratio

Maximum to sum ratio M_n / S_n can be used as an explanatory tool to tell about the finiteness (existence) of the moment of given order, say p . It is a standard knowledge that the mean and variance of a given data are their first order and second order moment, respectively.

Using maximum to sum ratio, we will be able to tell whether the variance, which is the second order moment, of data is finite (exists) or infinite (does not exist). The p^{th} order partial sum and p^{th} order maximum are given by $S_n(p) = \sum_{i=1}^n |X_i|^p$ and $M_n(p) = \max(|X_1|^p, \dots, |X_n|^p)$, respectively.

From [5], we have the following equivalence relation

$$R_n(p) = M_n(p) / S_n(p) \rightarrow 0 \Leftrightarrow E |X|^p < \infty$$

This equivalence relation means that p^{th} order maximum to p^{th} order partial sum ratio goes to zero as n approaches infinity if and only if the p^{th} order moment exists.

A direct way to exploit the above fact is to plot the max to sum ratio for 1st or 2nd order moment, if the plot for a given moment order goes to zero, then we might say that the moment of that order is finite (exists). It is also to note that a heavy tail distribution with tail parameter $\alpha < 2$ has an infinite variance and if $\alpha < 1$, the mean also is infinite. In the first row first column in Figure 1, we see that internal Ethernet traffic data have a finite variance because the Maximum to Sum Ratio tends to zero very quickly. Notice that we have plotted only the first 400 values, which account for only a fraction of the data. Also from the Figure1, we see that the external traffic (2nd and 3rd row), represented by Oct89Ext and LFSN, have infinite variance but a finite mean.

Now that we have an idea about the different moments and structure of the traffic, it is time to look for the parent distribution that might have produced the data.

2.3 Probability Paper Plot

The idea behind probability paper plot (PPP) is to graphically check whether our sample could have come from the referenced distribution or not. The plot will look linear in case the sample matches the referenced distribution. A departure from linearity is a clear indication that the sample is not well approximated by the suggested distribution. Here we explain how does it work, then we apply it to the samples of traffic data. More details about this method can be found in [5].

2.4 Gumbel Plot

Gumbel plot is probability plot where the reference distribution is the Gumbel distribution. It is one of the most classical methods in extremes. It is a plot of the empirical distribution of the observed data against the theoretical quantiles of the Gumbel distribution. If the data come from Gumbel distribution then the plot will look linear, otherwise the plot shows a convex or concave curvature depending on whether data come from a distribution with a tail heavier than the Gumbel's or lighter, respectively. Gumbel plot method is close in spirit to the QQ and Probability plots. Gumbel plot method is also known as double logarithmic plot.

In Gumbel method, we plot the empirical quantiles versus the quantiles of the theoretical Gumbel distribution. The plot is given as

$\{X_{k,n}, -\ln(-\ln(p_{k,n}))\}, k = 1, \dots, n\}$, where $p_{k,n} = (n - k + 0.5) / n$ are plotting positions.

Four Gumbel plots are shown in Figure 2. These plots are based on the block maximum series of the data. Block maximum of internal LAN (second column) shows a concave curve deviation from straight line (theoretical Gumbel quantiles). This concave deviation suggests block maxima distribution with a lighter tail than Gumbel's. Meanwhile, the two other plots in the first column have a convex shape. This convex departure from linearity suggests block maxima traffic that follows an extreme Fréchet distribution. These statements are to be analyzed and confirmed by estimating model parameters. Remember that we are talking about the distribution of block maxima and not the whole traffic data.

2.5 Mean Excess Function

The mean excess function of a probability distribution is given as $e(u) = E(X - u | X > u), 0 \leq u < x_f$, where u is a given threshold and x_f is the support or right end point of the distribution.

Mean excess function is used under different names in different disciplines. In insurance, it is the expected claim size in the unlimited layer; in finance, it is the shortfall; in reliability, it is the mean residual life.

Mean excess plot (meplot) is based on the mean excess function. It is a useful visualization tool. It helps in discriminating in the tail of traffic data. If traffic data comes from a distribution with a heavier tail than Gumbel's, then the plot will look linearly increasing. If data come from a distribution with a lighter tail than the Gumbel, then the mean excess plot will be linearly decreasing.

As a graphical tool we use the mean excess plot, it is based on the estimate of mean excess function. Suppose that we have X_1, \dots, X_n , the sample mean excess is given as

$$e_n(u) = 1/F(u) \int_u^\infty F_n(y) dy$$

The graph $\{X_{k,n}, e_n(X_{k,n})\}$ is called the mean excess plot.

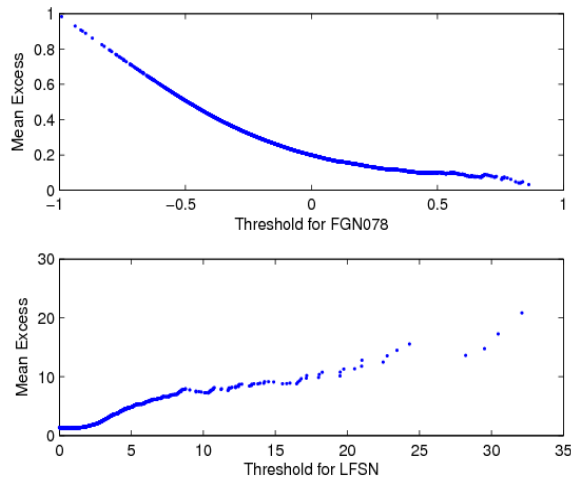


Fig. 3. Mean excess plots for FGN078(upper one) and LFSN

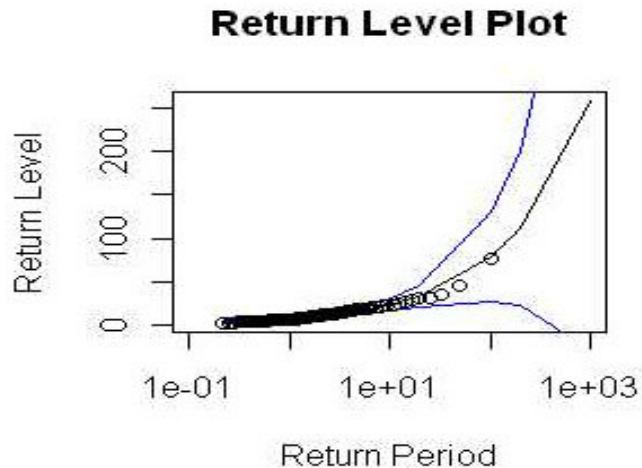


Fig. 4. Return level plot for LFSN.

Putting it together, we listed meplots for both internal and external simulated samples in Figure3. From the Figure, we see that the internal traffic has a decreasing meplot (upper one), while the external traffic has a linear increasing curve. These observations are in conformity with the theoretical Mean Excess function. The decreasing plot suggests a distribution with light tail. In the case of modeling with GEV, this behavior is analogous to a GEV with a negative shape parameter. The increasing plot suggests a distribution with heavier tail than Gumbel's. This increasing meplot is typical for a GEV with a positive shape parameter

3. MODEL PARAMETERS ESTIMATION

In general, to fit a model to the given data we need to estimate the parameters of that particular model, GEV model is no exception [3]. We chose the maximum likelihood (ML) method. ML method is implemented in the function *gev* from EVIM package [7]. We used blocks of size 100; this choice gives us maxima in blocks of 10 seconds each. We estimated model parameters using ML method.

From estimation results, we realized that internal traffic traces have negative shape parameter, while the two external traces have a positive shape parameter. This is an important observation since the shape parameter determines the type of fit distribution. In the internal traffic the negative shape parameter is an indication of the Weibull model. In external traffic case, the positive shape parameter is a clear indication of the traffic block maxima following an extreme Frechet distribution. Norros arrived at a similar conclusion for the internal traffic [14]. He showed analytically that the behavior of a buffer fed with internal traffic, approximated by fractional Gaussian noise, follows Weibull distribution. We arrived at a similar result but using extreme value theory perspective, which is much appropriate to the bursts prediction problem

4. PREDICTION

Apart from the model and its estimated parameters, we may use the powerful return level plot for the purpose of prediction. Return level plot is a plot of return period versus return level. We have produced a return level plot for the LFSN dataset with maxima taken in block of 100 observations. See Figure 4.

5. RESULTS AND ANALYSIS

Using EVT based model selection tools and parameters' estimates, we classify traffic bursts (block maxima) as coming either from a GEV distribution with positive shape parameter or GEV with a negative shape parameter, depending on the type of traffic.

From the EVT-based exploratory tools we notice that records of both kinds of traffic are within the confidence bounds of records from i.i.d data. This allows us to model the data not differently from i.i.d case. The max/sum ratio also is a good tool for discriminating the two types of traffic (internal/external). For the external traffic, since the plot for the second moment does not approach zero quickly we say the variance is infinite. From the right column plot, we say that the mean is finite. This is also an obvious observation since the plot of the ratio for the first moment tends to zero quickly. Same thing can be said on the mean of the internal traffic. However, unlike the external traffic, the internal traffic has finite variance.

The internal traffic, which is approximated by fractional Gaussian model, has traffic maxima that follows GEV model with negative shape parameter. Put differently, those block maxima fall in the Weibull domain of attraction.

The external traffic is best approximated by linear fractional stable noise (LFSN). This LFSN traffic model has block maxima that follow a GEV with a positive shape parameter. The same way as for internal traffic, this GEV with positive shape parameter means that bursts or traffic maxima fall in the domain of attraction of Extreme Frechet model.

Using extreme value distribution we are able to model the bursts or traffic maxima. This modeling of bursts is a valuable one. It permits us, in the context of Quality of Service, to define new extreme traffic metrics to be included in the Service Level Agreement (SLA) contracts. This will help service providers to deliver a better service to their clients, and the latter to ask for the service they actually need.

6. CONCLUSION

We used extreme value theory to the bursts prediction problem. In particular, we used Generalized Extreme Value model. Using EVT based model selection tools, traffic is seen to be naturally classified into external and internal traffic, following GEV model with positive and negative shape parameter, respectively. Model selection tools have further improved our confidence in the model. EVT as a framework is better suited than any other analytical model to predict bursts and serious deterioration in network traffic. It is computationally less expensive and requires minimum disk space. In future, we should consider assessing the fit of the model with some quality of fit measures.

7. REFERENCES

1. Patrice Abry and Fabrice Sellan. *"The wavelet-based synthesis for fractional Brownian motion proposed by F. Sellan and Y. Meyer: Remarks and fast implementation"*. Applied and Computational Harmonic Analysis, 3(4):377-383, 1996.
2. N. Balakrishnan, Jose Maria Sarabia, Enrique Castillo and Ali S. Hadi. *"Extreme Value and Related Models with Applications in Engineering and Science"*. Wiley, Wiley, 2004.
3. George Casella and Roger L. Berger. *"Statistical Inference"*. Duxbury, Pacific Grove, CA 93950, USA, 2001.
4. Abdelmahmoud Youssouf Dahab, Halabi Hasbullah and Abas Md Said, *"Predicting Traffic Bursts Using Extreme Value Theory"*. In International Conference on Signal Acquisition and Processing, pp.229-233, 2009.
5. Paul Embrechts, Thomas Mikosch and Claudia Klüppelberg. *"Modelling Extremal Events: for Insurance and Finance"*. Springer-Verlag, London, UK, 1997.
6. Hifang Feng and Yantai Shu. *"Study on network traffic prediction techniques"*. International Conference on Wireless Communications, Networking and Mobile Computing, 2005, 2(23-26 Sept. 2005):1041–1044, September 2005.
7. Ramazan Genay, Faruk Seluk, and Abdurrahman Uluglyagci. *"Evim: A software package for extreme value analysis in matlab"*. Studies in Nonlinear Dynamics & Econometrics, 5(3):1080–1080, 2001.
8. A. Karasaridis and D. Hatzinakos. *"Network heavy traffic modeling using alpha-stable self-similar processes"*. Communications, IEEE Transactions on, 49(7):1203–1214, Jul 2001.
9. M. R. Leadbetter and Holger Rootzen. *"Extremal Theory for Stochastic Processes"*. The Annals of Probability. 16(2):431-478, 1988.
10. M. Li and S. C. Lim. *"Modeling network traffic using generalized Cauchy process"*. Physica A, 387(11): 2584-2594, 15 April 2008.
11. M. Li and W. Zhao. *"Representation of a Stochastic Traffic Bound, accepted for publication"*. IEEE Transactions on Parallel and Distributed Systems, 2009.
12. Chunfeng Liu, Yantai Shu, and Jiakun Liu. *"Application of Extreme Value Theory to the Analysis of Wireless Network Traffic"*. In Proceedings of IEEE International Conference on Communications, ICC 2007, Glasgow, Scotland, 24-28 June 2007.
13. Abuagla Babiker Mohd and Sulaiman bin Mohd Nor. *"Towards a Flow-based Internet Traffic Classification for Bandwidth Optimization"*. International Journal of Computer Science and Security (IJCSS), 3:2, 146-153. 2009.
14. Ilkka Norros. *"On the use of fractional brownian motion in the theory of connectionless networks"*. IEEE Journal of Selected Areas in Communications, 13(6):953–962, 1995.
15. Kihong Park and Walter Willinger. *"Self-Similar Network Traffic and Performance Evaluation"*. John Wiley & Sons, New York, USA, 2000.
16. Gennady Samorodnitsky and Murad S. Taqqu. *"Stable Non-Gaussian Random Processes: Stochastic Models with Infinite Variance"*. Chapman & Hall, London SE1 8HN, 1994.
17. Stilian Stoev and Murad S. Taqqu. *"Simulation methods for linear fractional stable motion and farima using the fast fourier transform"*. Fractals, 12:2004, 2004.

18. Zoi Tsourti and John Panaretos. “*Extreme-value analysis of teletraffic data*”. Computational Statistics Data Analysis, 45(1):85 – 103, 2004. Computer Security and Statistics.

19. M. Uchida. “*Traffic data analysis based on extreme value theory and its applications*”. Global Telecommunications Conference, 2004. GLOBECOM’04. IEEE, 3:1418–1424 Vol.3, Nov.-3 Dec. 2004.

20. Wei Biao Wu, George Michailidis, and Danlu Zhang. “*Simulating sample paths of linear fractional stable motion*”. IEEE Transactions on Information Theory, 50:1086–1096, 2004.

21. Internet traffic Archive, “<http://ita.ee.lbl.gov>”.

BIOGRAPHY

1. Abdelmahamoud Youssouf Dahab is a PhD candidate in Computer & Information Sciences Department, Universiti Teknologi PETRONAS.

2. AP Dr Abas Md Said is a lecturer in the Computer and Information Sciences Department at Universiti Teknologi PETRONAS. He obtained his Bachelor and Masters of Science from Western Michigan University, USA. Doctor of Philosophy from Loughborough University, UK. He specializes in Computer Graphics, Visualization, and Networks. His research interests are in Optimized Stereoscopic Rendering for Visualization. He has a number of publications.

3. Dr Halabi Hasbullah is a lecturer in the Computer and Information Sciences Department at Universiti Teknologi PETRONAS. He obtained his Bachelor of Science (Mathematics) from Universiti Malaya, Malaysia. His Masters of Science (Information Technology) from De Montfort University, UK. And PhD (Communications System), National University of Malaysia (UKM), Malaysia. He specializes in Network Communications. His research interests are Bluetooth network, Traffic engineering, Wireless sensor network (WSN), Vehicular ad hoc network (VANET), and IPv6. He has a number of publications.

Investigating the Effect of Mutual Coupling on SVD Based Beamforming over MIMO Channels

Feng Wang

*School of Information Technology & Electrical Engineering
University of Queensland
Brisbane, 4072, Australia*

fwang@itee.uq.edu.au

Marek E. Bialkowski

*School of Information Technology & Electrical Engineering
University of Queensland
Brisbane, 4072, Australia*

meb@itee.uq.edu.au

Xia Liu

*School of Information Technology & Electrical Engineering
University of Queensland
Brisbane, 4072, Australia*

xialiu@itee.uq.edu.au

Abstract

This paper reports on investigations into a narrowband Multiple-Input Multiple-Output (MIMO) system that applies the Singular Value Decomposition (SVD) beamforming over a Rician channel. Assuming that the two sides of the communication link have a perfect knowledge of Channel State Information (CSI), the system applies the SVD-based beamforming both at the transmitter and receiver. The assessment of the system performance takes into account Mutual Coupling (MC) that is present in the transmitting and receiving array antennas. It is shown that for some particular ranges of Signal to Noise Ratio (SNR) and inter-element spacing, mutual coupling can increase the capacity and thus can be beneficial in terms of decreasing Symbol Error Rate (SER).

Keywords: MIMO, Mutual Coupling, SVD, Beam-forming, LMMSE.

1. INTRODUCTION

Multi-Input Multi-Output (MIMO) systems employing multiple element antennas (MEAs) both at the transmitter and receiver have been proved to offer a significant capacity gain over traditional Single-Input Single-Output (SISO) systems in rich scattering environments [1] [2]. Because of this attribute, the MIMO technique is regarded as one of the most promising techniques for future wireless communications and as such it has received a significant attention from academia and industry in the last decade.

Initial investigations into MIMO systems were carried out by researchers working in the field of information theory [1] [2]. They have shown that the MIMO technique can provide an increased system capacity under Non-Line of Sight (NLOS) signal propagation conditions when the channel

matrix is formed by Independent Identically Distributed (*i.i.d.*) complex Gaussian entries [1]. In practice, the properties of an actual wireless channel differ from the *i.i.d.* conditions, as signals experience both NLOS and Line Of Sight (LOS) signal propagation paths.

In order to exploit the potential of MIMO, different transmission schemes have been proposed. It has been shown that if the Channel State Information (CSI) is available only at the receiver, Space-time coding [3] [4] can offer considerable benefits to the operation of MIMO system. However, when full or partial CSI is available at the transmitter, a directional beamforming can be a more viable signal transmission scheme [5] [6] [7]. This is because it can increase the average received Signal to Noise Ratio (SNR) due to the array antenna gain. Such benefits have been proved for the case of significant LOS path existing between the transmitter and receiver. However, when NLOS conditions dominate the signal propagation environment, the directional beamforming becomes inferior because of absence of the well defined “desired direction”. In this case, a Singular Value Decomposition (SVD) based beamforming is an attractive alternative. This is because it can better exploit the spatial properties of MIMO channel. When CSI is available at the transmitter and receiver sides, the SVD based beamforming accompanied by linear transmit-receive processing enables transmission of symbols over the eigenmodes of the MIMO channel [2]. This type of signal transmission is often referred to as Multichannel Beam-forming (MB) [9]. In [8], the Schur-concave and Schur-convex functions have been used to design the double beamforming system in which beamforming is applied both at the transmitter and receiver. It has been shown that the channel-diagonalized MB is an optimal transmission scheme. In [10], investigations have been carried out into the combined transmission scheme involving the space-time coding and the SVD based Multichannel Beamforming.

It is worthwhile to note that all of these works have been accomplished using the assumption of “ideal array antennas”, in which many practical issues such as the array geometry and orientation, and the effect of mutual coupling due to finite element spacing are not taken into account. It is known that Mutual Coupling (MC) is always present in multi-element antennas and its effect cannot be ignored especially in tightly spaced arrays. The problem of Mutual Coupling in relation to MIMO systems has been reported in [11] [12] [13] [14]. In [12], the effect of MC has been investigated in relation to the interference rejection capabilities of Beamforming arrays. As a follow up of investigations in [11] and [12], the work in [14] has considered the impact of mutual coupling on the information rate (capacity) when the beamforming signal transmission scheme is applied over a Rician MIMO channel. In this paper, the impact of mutual coupling is investigated with regard to the SVD based multichannel beamforming.

The paper is structured as follows. In section 2, the system model is introduced. Section 3 describes the SVD based multichannel beamforming transmission scheme. The mutual coupling effect is modeled in section 4. The analysis concerning the effect of mutual coupling on the SVD based multichannel beamforming, including numerical results, is presented in section 5. Section 6 concludes the paper and gives suggestions for a future work.

2. SYSTEM MODEL

2.1 MIMO system with double beam-forming

The investigation is undertaken for a flat block-fading narrow-band MIMO system equipped with N transmitting antennas and M receiving antennas both applying the beamforming strategy. For this system, the received baseband signal can be represented as

$$\mathbf{r} = \mathbf{H}\mathbf{s} + \mathbf{n} \quad (1)$$

where $\mathbf{r} \in \mathbb{C}^{M \times Q}$ is the received signal matrix, $\mathbf{H} \in \mathbb{C}^{M \times N}$ is the complex channel matrix, $\mathbf{s} \in \mathbb{C}^{N \times Q}$ is the transmitted symbol matrix, and $\mathbf{n} \in \mathbb{C}^{M \times Q}$ is the zero-mean circularly symmetric complex Gaussian noise matrix with power spectral density of $\sigma^2/2$ per element.

Assuming that the transmitter applies the beamforming scheme, the transmitted signal vector can be written as

$$\mathbf{s} = \mathbf{W}_T \mathbf{x} \tag{2}$$

where $\mathbf{W}_T \in \mathbb{C}^{N \times P}$ is the transmit beamforming matrix and $\mathbf{x} \in \mathbb{C}^{P \times Q}$ is the output symbol matrix of the space-time encoder with $P \leq \min(M, N)$. The input information symbols are of the form $\mathbf{Z} = (z_1, z_2, \dots, z_L)$, $L \leq PQ$.

To keep the transmit power constant, the following condition is imposed

$$\mathbf{W}_T^H \mathbf{W}_T = \mathbf{I}_{P \times P} \tag{3}$$

The signal matrix estimated at the receiver is given by

$$\mathbf{y} = \mathbf{W}_R^H \mathbf{r} \tag{4}$$

where $\mathbf{y} \in \mathbb{C}^{P \times Q}$ is the estimated matrix of $\mathbf{x} \in \mathbb{C}^{P \times Q}$ and $\mathbf{W}_R \in \mathbb{C}^{P \times M}$ is the receiving beamforming matrix. Each column of \mathbf{W}_R can be interpreted as a beamvector adapted to each spatial sub-channel.

2.2 Channel model

It is assumed that array antennas at the transmitter and receiver are formed by linear parallel wire dipoles. The distance between the transmitting and receiving arrays is given by D and an angle between their axes is θ . The received signal is assumed to include both LOS and NLOS components. As a result, the elements h_{rt} of the channel matrix \mathbf{H} representing the transfer function or channel response between the t^{th} transmitting element and the r^{th} receiving element are given by [11][15]

$$h_{rt} = \sqrt{\frac{1}{1+K}} h_{rt}^{NLOS} + \sqrt{\frac{K}{1+K}} h_{rt}^{LOS} \tag{5}$$

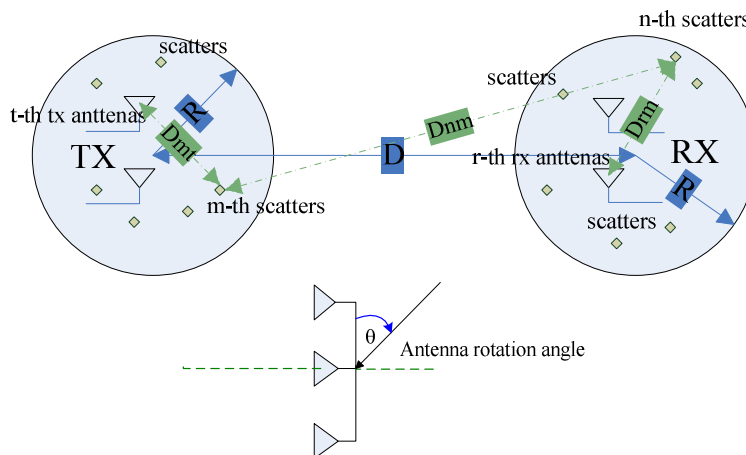


FIGURE 1: Configuration of the investigated MIMO system showing relative orientation of the transmitting and receiving array antennas and a two ring double-bounce scattering signal propagation model.

In the above expression, K is the Rician factor, which is defined as the power ratio between the LOS and NLOS components. The LOS component is represented by

$$h_{rt}^{LOS} = \exp(-j \frac{2\pi}{\lambda} d_{rt}) \quad (6)$$

and the NLOS component is given by

$$h_{rt}^{LOS} = \sqrt{\frac{1}{S_R S_T}} \sum_{m=1}^{S_T} \sum_{n=1}^{S_R} \alpha_{mn} \exp(-j \frac{2\pi}{\lambda} (d_{mt} + d_{nm} + d_{rn})) \quad (7)$$

in which α_{mn} is the scattering coefficient for the path between the m^{th} scatterer at the transmitter side and the n^{th} scatterer at the receiver. This coefficient is assumed to be represented by a normal complex random variable with zero mean and unit variance. d_{rt} is the distance between the t^{th} transmitting antenna and the r^{th} receiving antenna and d_{nm} is the distance between the m^{th} and n^{th} scatterers. d_{mt} is the distance between the m^{th} scatterer and t^{th} transmit antenna. d_{rn} is the distance between the r^{th} receiving antenna and the n^{th} scatterer. It is assumed that S_R scatterers surround the receiver and S_T scatterers encircle the transmitter. Also it is assumed that H is known both to the receiver and transmitter and thus perfect CSI is available at the two sides of the communication link.

3. SVD BASED BEAMFORMING WITH BEAM SELECTIONS

By applying the Singular Value Decomposition (SVD) [16], the MIMO channel matrix $\mathbf{H} \in \mathbb{C}^{M \times N}$ can

be represented in the following form [10]

$$\mathbf{H} = \mathbf{U} \mathbf{\Sigma} \mathbf{V}^H$$

$$= \underbrace{[\mathbf{u}_1 \cdots \mathbf{u}_M]}_{\mathbf{U}} \underbrace{\begin{bmatrix} \sigma_1 & & & & & \\ & \ddots & & & & \\ & & \sigma_M & 0 & \cdots & 0 \end{bmatrix}}_{\mathbf{\Sigma}} \underbrace{[\mathbf{v}_1 \cdots \mathbf{v}_N]}_{\mathbf{V}}^H \quad (8)$$

where σ_m is the m^{th} non-negative singular value from a set of $\sigma_1 \geq \sigma_2 \geq \dots \geq \sigma_M$, \mathbf{U} and \mathbf{V} are the corresponding singular vector unitary matrices, $\mathbf{U}^H \mathbf{U} \in \mathbb{C}^{M \times M}$ and $\mathbf{V}^H \mathbf{V} \in \mathbb{C}^{N \times N}$. $(\cdot)^H$ denotes the hermitian operation which implies the transposed complex conjugate of the argument. \mathbf{V} is the matrix with the columns given by the eigenvectors of $\mathbf{H}^H \mathbf{H}$, which are related to the eigenmodes of the MIMO channel matrix

$$(\mathbf{H}^H \mathbf{H}) \mathbf{V} = \mathbf{V} (\mathbf{\Sigma}^H \mathbf{\Sigma}) \quad (9)$$

As assumed earlier, perfect CSI is available at both the receiver and transmitter. Under this assumption, the maximum capacity is achieved by transmitting independent Gaussian codes on the eigenmodes with water-filling power allocation strategy [1] [9].

The SVD-based multichannel beamforming technique exploits the MIMO channels' eigenmodes by employing P ($P \leq M$ and $P \leq N$) columns of matrix \mathbf{V} which correspond to the P largest eigenmodes (alternatively named singulars). Therefore the transmit beamforming matrix is given by

$$\mathbf{W}_T = \mathbf{V}^P \text{ and } \mathbf{s} = \mathbf{V}^P \mathbf{x} \quad (10)$$

In order to represent the received signals in terms of eigenmodes, expression (8) is used and leads to the following

$$\begin{aligned}
 \mathbf{y} &= \mathbf{U}_p^H \mathbf{r} \\
 &= \mathbf{U}_p^H \mathbf{H} \mathbf{V}_p \mathbf{x} + \mathbf{U}_p \mathbf{n} \\
 &= \mathbf{\Sigma}_{P \times P} \mathbf{x}
 \end{aligned} \tag{11}$$

It is important to note that this beamforming method does not always result in a robust transmission scheme, especially when the transmitter has only an approximate knowledge of CSI. This shortfall can be compensated by a beamforming performed at the receiver. The optimal receive beamforming matrix can be obtained by selecting one of the sub-streams' minimum mean square error (MMSE) as the cost function. This results in the *Wiener solution*. Receivers employing the beamforming matrix based on the *Wiener solution* are named LMMSE receivers. The receive beamforming matrix can thus be represented by

$$\mathbf{W}_R = (\mathbf{H} \mathbf{V}_p \mathbf{V}_p^H \mathbf{H}^H + \mathbf{I}_n)^{-1} \mathbf{H} \mathbf{V}_p \tag{12}$$

The MIMO channel matrix \mathbf{H} can be decomposed into P parallel independent sub-channels, each sub-channel bearing one symbol from the transmitted signal matrix. The received signal matrix can be written as

$$\mathbf{y} = \mathbf{W}_R^H \mathbf{H} \mathbf{W}_T + \mathbf{W}_R^H \mathbf{n} \tag{13}$$

The equivalent scalar form of (13) is given by

$$y_{pq} = \varepsilon \sqrt{d_p} x_{pq} + n_p, 1 \leq p \leq P \text{ and } 1 \leq q \leq Q \tag{14}$$

where $\varepsilon = 1/(K+1)^{0.5}$, y_{pq} is the estimated symbol in the p^{th} row, q^{th} column of the signal matrix, n_p is the p^{th} elements of \mathbf{n} , d_p is the p^{th} largest eigen-value of

$$\mathbf{\Gamma} = (\varepsilon^2 \mathbf{I}_s)^{-1} \mathbf{H}^H \mathbf{H} \tag{15}$$

4. SVD based beamforming with mutual coupling

4.1 Modeling of mutual coupling

For the array formed by linear parallel wire dipoles, the mutual coupling matrix can be expressed by [12]

$$\mathbf{C} = (\mathbf{Z}_A + \mathbf{Z}_T)(\mathbf{Z} + \mathbf{Z}_T \mathbf{I}_M)^{-1} \tag{16}$$

where Z_A is the element impedance in isolation and Z_T is the impedance of the receiver at each element, and is chosen as the complex conjugate of Z_A to obtain the impedance match. \mathbf{Z} is the mutual impedance matrix with all the diagonal elements equal to $Z_A + Z_T$. Its non-diagonal elements Z_{nm} are dependent on the physical parameters of dipoles including length, and distance between them. For a side-by-side array configuration and dipole length equal to 0.5λ , Z_{nm} is given by [11] [12]

$$Z_{mn} = \begin{cases} 30[0.5722 + \ln(2\beta l) - C_i(2\beta l)] + j[30S_i(2\beta l)], & m = n \\ 30[2C_i(u_0) + C_i(u_1) - C_i(u_2)] + j[302S_i(u_0) - S_i(u_1) - S_i(u_2)] & m \neq n \end{cases} \tag{17}$$

where

$$C_i(u) = \int_{\infty}^u \frac{\cos(x)}{x} dx$$

$$S_i(u) = \int_0^u \frac{\sin(x)}{x} dx$$
(18)

and the constants are given by [13]

$$u_0 = \beta d_h$$

$$u_1 = \beta \left(\sqrt{d_h^2 + l^2} + l \right)$$

$$u_2 = \beta \left(\sqrt{d_h^2 + l^2} - l \right)$$
(19)

where d_h is the horizontal distance between the two dipole antennas.

4.2 Effect of mutual coupling on SVD based beamforming

The earlier derived expressions (13) describing the operation of the SVD based beamforming system neglect mutual coupling. The inclusion of mutual coupling is straight forward and can be accomplished by modifying the earlier assumed channel matrix \mathbf{H} to \mathbf{H}_{mc} . As a result, the operation of the SVD based beam-forming system that takes into account the mutual coupling present in the transmitting and receiving array antennas is described by

$$\mathbf{y} = \mathbf{W}_R^H \underbrace{\mathbf{C}_R \mathbf{H} \mathbf{C}_T}_{\mathbf{H}_{mc}} \mathbf{W}_T + \mathbf{W}_R^H \mathbf{n}$$
(20)

where \mathbf{C}_R and \mathbf{C}_T represent the mutual coupling at receiver and transmitter respectively.

It is apparent that when the mutual coupling effect is neglected (the case of an ideal antenna array), the mutual coupling matrices are given by unit matrices

$$\mathbf{C}_R = \mathbf{I}_{M \times M} \quad \text{and} \quad \mathbf{C}_T = \mathbf{I}_{N \times N}$$
(21)

The new channel matrix \mathbf{H}_{mc} that includes mutual coupling effects can be decomposed by the SVD technique to

$$\mathbf{H}_{mc} = \mathbf{C}_R \mathbf{H} \mathbf{C}_T$$

$$= \mathbf{U}_{mc} \boldsymbol{\Sigma}_{mc} \mathbf{V}_{mc}^H$$
(22)

The \mathbf{H}_{mc} matrix dimensions are the same as of the original matrix \mathbf{H} which neglects the mutual coupling. Due to the presence of mutual coupling, the channel characteristics are changed and the unitary property does not hold any more

$$\mathbf{U}_{mc}^H \mathbf{U}_{mc} \neq \mathbf{I}_{M \times M}$$

$$\mathbf{V}_{mc} \mathbf{V}_{mc}^H \neq \mathbf{I}_{N \times N}$$
(23)

This means that it is impossible to perfectly separate the received signal into different eigenmodes. This property is named as “cross talk” between eigenmodes [17].

5. NUMERICAL RESULTS

The performance of the SVD based beamforming technique including mutual coupling is assessed via Monte-Carlo simulations. The effect of the Rician factor K and the receive antenna spacing is investigated. Equations (5), (6) and (7) are used to model the channel matrix \mathbf{H} . The transmitting and receiving array antennas are assumed parallel one to each other and thus the

orientation angle θ is equal to 0° . The distance, D , between the transmitter and the receiver is assumed to be 50λ and the rings enclosing the array antennas are of radius R equal to 16λ , where λ is the carrier wavelength. $S_R=S_T= 50$ scatterers are assumed to be uniformly distributed in the two rings surrounding the transmitting and receiving array antennas.

Since the SVD based multichannel beamforming utilizes the MIMO channels' eigenmodes (singulars) to transmit signals, it is important to investigate their statistical properties. Figure 2 shows the cumulative distributions for the sum of four singulars of a 4×4 Rician MIMO channel for different values of Rician factor K . Note that in this case, the sum of eigenvalues is related to the capacity of MIMO system. Simulations assume that the array rotation angle is equal to 0° , which means that the signals are transmitted and received in the broadside direction. The inter-element spacing is 0.5λ . Two cases are considered when the mutual coupling is neglected (continuous blue lines) and when the mutual coupling is taken into account (dashed red lines).

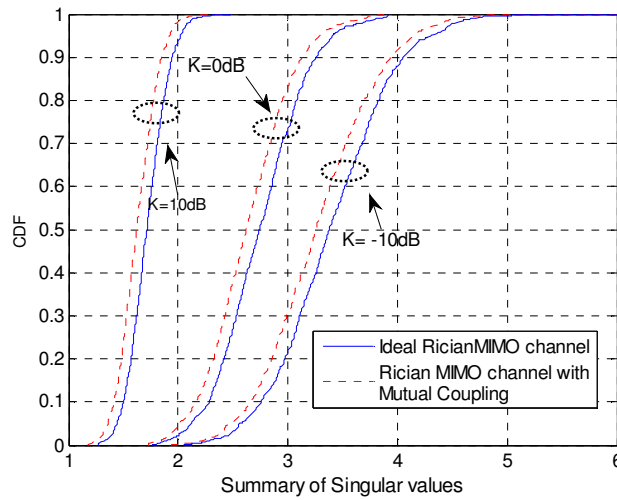


FIGURE 2: CDF of Sum of Singular values for 4×4 MIMO.

It is apparent from the results presented in Figure 2 that irrespective of the value of the Rician factor K , larger sums of singular values indicating a larger capacity are for the case without mutual coupling (blue lines).

Figure 3, Figure 4 and Figure 5 show the probability density of the individual singular values of the 4×4 MIMO channel for different values of Rician factor $K=-10\text{dB}$, 0dB and 10dB .

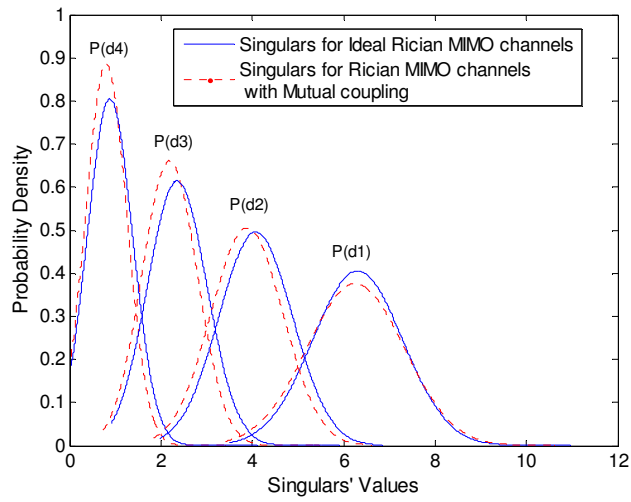


FIGURE 3: PDF of Singular values for 4x4 MIMO ($K= -10\text{dB}$).

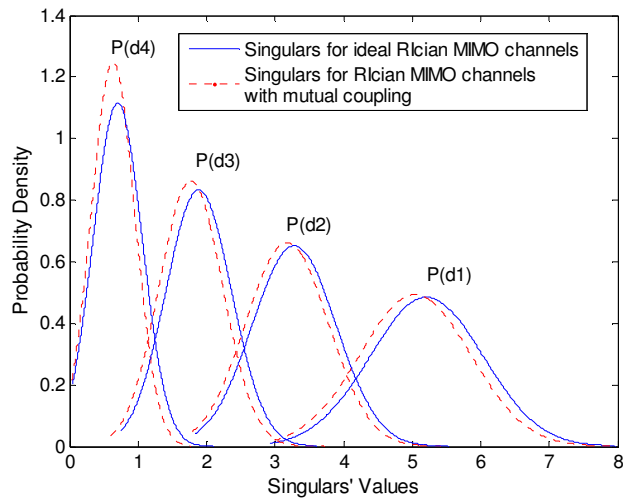


FIGURE 4: PDF of Singular values for 4x4 MIMO ($K= 0\text{dB}$).

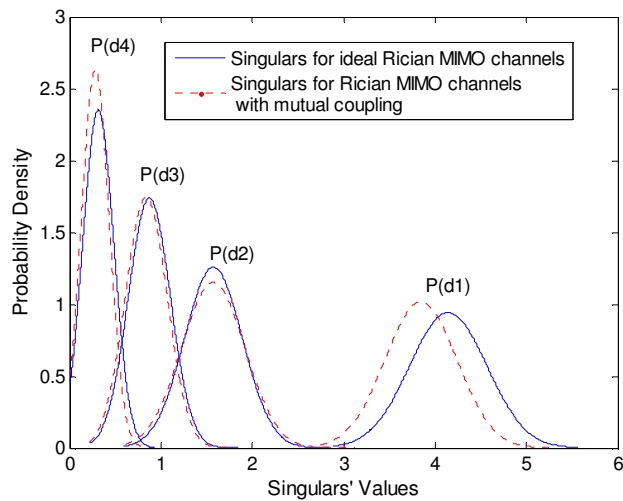


FIGURE 5: PDF of Singular values for 4x4 MIMO ($K= 10\text{dB}$).

It can be seen from the results presented in Figures 3, 4 and 5 that when the mutual coupling effect is taken into consideration (dashed red lines) the singulars are slightly shifted to the left with respect to the singulars when mutual coupling is neglected (continuous blue lines). This shift is caused by the impedance mismatch causing the drop of the singular values. This result is consistent with the results shown in Figure 2. Also seen from the presented figures is that the singulars values show different probability properties for different values of K . When $K = -10\text{dB}$, meaning that NLOS component dominates the Rician channel, all the singular values probability density plots have crossing points with their neighbours. When $K = 10\text{dB}$, meaning that the LOS component dominates the Rician channel, the largest singular value is isolated from the other singular values. This indicates that the largest singular value establishes the dominant position when K is considerably increased.

Figure 6 shows the capacity as a function of SNR for the SVD based beamforming system with a LMMSE receiver operating over a 4×4 MIMO Rician channel. When $K = -10\text{dB}$, meaning that NLOS component dominates the Rician channel, the two capacity plots for the SVD based beamforming with and without mutual coupling cross at 19.35dB . At higher SNR ($\text{SNR} > 19.35\text{dB}$) the mutual coupling degrades the capacity performance. At lower SNR, ($\text{SNR} < 19.35\text{dB}$) mutual coupling increases the capacity. When $K = 10\text{dB}$, meaning that LOS component dominates the Rician channel, one can see that the red dashed lines are always below the blue ones, which means that the mutual coupling degrades the capacity.

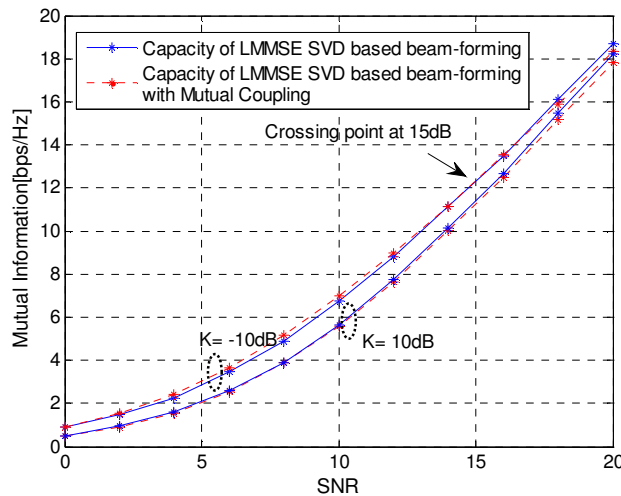


FIGURE 6: Capacity of SVD based beam-forming with LMMSE receiver for

a 4×4 Rician MIMO channels (Inter-element spacing is equal to 0.5λ).

Figure 7 shows the capacity of SVD based beam-forming system with LMMSE receiver operating for over a 4×4 MIMO Rician channel for a varying inter-element spacing.

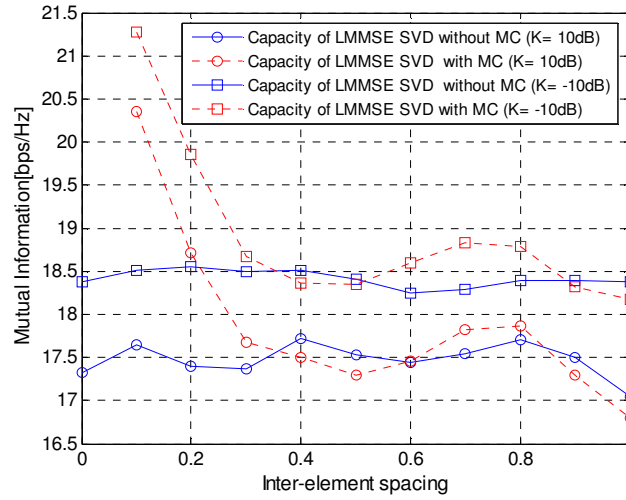


FIGURE 7: Capacity of SVD based beam-forming with LMMSE receiver for a 4×4 Rician MIMO channels

(SNR is equal to 20dB; Inter-element spacing transmitter is 1.0λ).

One can see that there are three crossing points for the two plots with and without mutual coupling. For $K = 10\text{dB}$, the plots with and without mutual coupling cross at 0.35λ , 0.6λ and 0.85λ . In the range of inter-element spacing from 0 to 0.35λ and from 0.6λ to 0.85λ , mutual coupling increases the capacity. For $k = -10\text{dB}$, the curves show the same trend, although the crossing points' locations are slightly different. From the results presented in Figure 7 it is apparent that the largest differences in mutual information are observed for the inert-element spacing less than 0.35λ .

Figure 8 shows the SER performance for SVD based beamforming with LMMSE receiver for a 2×2 MIMO Rician channel. The Alamouti coded SVD based beam-forming is applied [4].

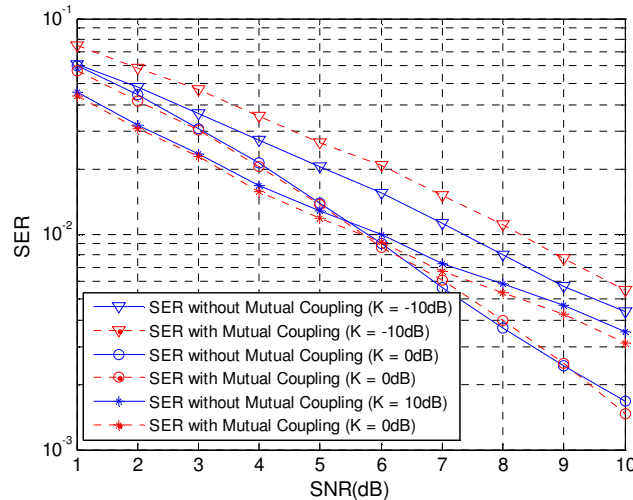


FIGURE 8: SER performance of Alamouti coded SVD based beam-forming with LMMSE receiver for a 2×2

Rician MIMO channels (Inter-element spacing for transmitter and receiver array are 1.0λ and 0.5λ).

The presented plots in Figure 8 show that the Alamouti coded SVD based beamforming with LMMSE receiver has a better SER performance in a scattering-rich environment. This is when the Rician factor takes smaller values. Also it can be seen that the effect of mutual coupling on SER performance depends on the signal propagation environment. When $K = 10\text{dB}$, the LOS component dominates the channel, mutual coupling is beneficial in terms of decreasing SER. This drop can be attributed to the decreased correlation between different antenna elements. When $K = -10\text{dB}$ and the NLOS component dominates the channel, the “cross talk” effect becomes non-negligible and the presence of mutual coupling leads to an increased SER. When NLOS and LOS components are comparable ($K = 0\text{dB}$), the SER plots for SVD based beamforming with and without mutual coupling have a cross-point at some value of SNR. At higher SNR, mutual coupling contributes to a better SER performance while at lower SNR mutual coupling is responsible for decreasing the SER performance.

6. CONCLUSIONS

In this paper, investigations have been performed into the SVD based multichannel beamforming technique which takes into account the effects of mutual coupling present in transmitting and receiving array antennas. In these investigations, the transmitting and receiving antennas have been assumed to be in the form of uniform arrays of parallel wire dipoles that are surrounded by circular rings of uniformly distributed scattering objects. In the analysis, it has been postulated that the communication link includes both Line-of-Sight and Non-line of Sight signal propagation paths. The mutual coupling has been taken into account by modifying the channel matrix by the transmitting and receiving antenna coupling matrices.

The assessment of this Multiple-Input Multiple-Output system has been performed via computer simulations assuming different values of the Rician factor and different values of inter-element antenna spacing. The presented simulation results have shown that for some particular ranges of SNR and inter-element spacing, mutual coupling can increase the capacity. Also it can contribute to a better SER performance.

7. REFERENCES

1. G. J. Foschini, M. J. Gans, “*On Limits of Wireless Communication in a Fading Environment when Using Multiple Antennas*”, Int J. Wireless Personal Communications, no.6, pp.311-335, 1998
2. I. E. Telatar, “*Capacity of Multi-antenna Gaussian Channels*”, Euro Trans. on Telecommunications, no.10, pp.585-595, 1999
3. V. Tarokh, N. Seshadri and A. R. Calderbank, “*Space-time Codes for High Data Rate Wireless Communications: Performance Criterion and Code Construction*”, IEEE Trans. Inform. Theory, vol.44, pp.744-765, March 1998
4. A. M. Alamouti, “*A Simple Transmit Diversity Technique for Wireless Communication*”, IEEE Journal on Selected Areas in Communication, vol.16, pp.1451-1458, Oct 1998.
5. Yongzhao Li, Feng Wang and Guisheng Liao, “*Space-time Coded Eigenbeamforming for Wireless Downlink Transmission*”, in IEEE Proc. of International Conference on Signal Processing, Beijing, China, 2004.
6. G. Jongren, M Skoglund and B. Ottersten, “*Combining Beamforming and Orthogonal Space-time Block Coding*”, IEEE Trans. on Information and Theory, vol.48. No.3 Mar.2002
7. J. Liu, E. Gunawan, “*Combining ideal beamforming and Alamouti space-time block codes*”, IEEE Electronic Letters, vol. 39, No.17, August 2003
8. D. P. Palomar, J. M. Goffi and M. A. Lagunas, “*Joint Tx-Rx Beamforming Design for Multicarrier MIMO Channels: A Unified Framework for Convex Optimization*”, IEEE Trans. Signal Processing, vol.51, pp.2381-2401, September 2003
9. Shi Jin, R. McKay, X.Q. Gao and J.B. Collings, “*MIMO Multichannel Beamforming: SER Outage Using New Eigenvalue Distributions of Complex Noncentral Wishart Matrices*”, IEEE Trans. on Comm. Vol56, No.3 March 2008

10. F. Wang, X. Liu and M. E. Bialkowski, "*Investigations into Space-time Coded SVD Based Beamforming for a MIMO System*". In Proc. of the International Conference on Advanced Inforcomm Technology. Xi'an, Shaanxi, China, 2009
11. M. E. Bialkowski, P. Uthansakul, K.Bialkowski and S. Durrani, "*Investigating the Performance of MIMO Systems from an Electromagnetic Perspective*", Microwave and Optimal Technology Letters, vol.48, No.7, pp. 1233-1238, July 2006
12. S. Durrani, M. E. Bialkowski, "*Effect of Mutual Coupling on the Interference Rejection Capabilities of Linear and Circular Arrays in CDMA Systems*", IEEE Trans. on Antennas and Propagation, vol.52, No.4, pp. 1130-1134, April 2004.
13. B.Clerck, D.V Janiver, C. Oestges and L. Vandendorpe, "Mutual Coupling Effects on the Channel Capacity and the Space-time Processing of MIMO Communications Systems", in Proc. of ICC Conf, pp2638-2964. 2003.
14. F. Wang, X. Liu and M. E. Bialkowski, "*Performance of MIMO Beamforming Transmission Scheme in the Presence of Mutual Coupling-final*". Submitted to Asia-Pacific Microwave Conference. Singapore,2009
15. P. Uthansakul, M.E. Bialkowski, S. Durrani, K. Bialkowski, and A. Postula, "*Effect of Line of Sight Propagation on Capacity of an Indoor MIMO System*", In Proc. of IEEE Int Antennas Propagat. Symp, Washington, DC, 2005.
16. Gene H.G., Charles F.V., *Matrix Computation(3^d Edition)*, Johns Hopkins University Press, Baltimore, MD, 1996
17. D.N. Nissani, "*About SVD Based MIMO, Imperfect Channel Estimates, and Cross-talk Interference*" IEEE Proceedings of VTC 2006, pp1-5, Sep 2006

OFDM-CPM Performance and FOBP under IEEE802.16 Scenario

Alimohammad Montazeri

*Electrical Engineering Department
Iran University of Science and Technology
Tehran, Iran*

amm_montazeri@yahoo.com

Vahid Tabataba Vakily

*Electrical Engineering Department
Iran University of Science and Technology
Tehran, Iran*

vakily@iust.ac.ir

Abstract

The application of orthogonal frequency domain modulation-Continuous Phase Modulation (OFDM-CPM) in multipath Stanford University Interim (SUI) channels is presented in this paper. OFDM-CPM is proposed for IEEE 802.16 standards as an alternative technique of orthogonal frequency division multiplexing (OFDM) in physical layer. It is shown that, in addition to 0dB Peak to Average Power Ratio (PAPR) and power efficiency, un-coded OFDM-CPM exploits the frequency diversity of multipath channel. Taking into account the Input Power Back off (IBO), OFDM-CPM is shown to outperform OFDM at high bit energy-to-noise density ratios (E_b/N_0). However, at low Signal to Noise Ratio (SNR), the OFDM-CPM phase demodulator receiver suffers from a threshold effect. In addition, this paper compares the spectral fractional out of band power of OFDM-CPM for different modulation indices.

Keywords: OFDM-CPM, PAPR, SUI Multipath Channel Model, IEEE802.16, Fractional out of band power (FOBP).

1. INTRODUCTION

The future wireless communication networks will provide broadband services such as wireless Internet access to subscribers. Those broadband services require reliable and high-rate communications over time-dispersive (frequency-selective) channels with limited spectrum and inter-symbol interference (ISI) caused by multi-path fading. Orthogonal frequency division multiplex (OFDM) is one of the most promising solutions for a number of reasons. OFDM has high spectral efficiency since subcarriers overlap in frequency and adaptive coding and modulation can be employed across subcarriers. Its implementation is simplified because the base band modulator and demodulator are simply IFFT/FFT. Other advantages of OFDM include simple receiver (since only one tap equalizer is required) and excellent robustness in multi-path environment. Several variations of OFDM have been proposed as effective anti multipath techniques [1]. OFDM primarily offers a favourable trade-off between performance in severe multipath channels and signal processing complexity. OFDM is considered as physical layer transmission techniques for broadband wireless communication system. It has been adopted by HiperLAN/2, digital video broadcasting (DVB), digital audio broadcasting (DAB), IEEE 802.11a

wireless local area network (WLAN) standard, IEEE 802.16 wireless metropolitan area network (WMAN) standard[8]. Despite all the attractive advantages, OFDM has its disadvantages. OFDM has two primary drawbacks. The first is sensitivity to imperfect frequency synchronization. The second problem with OFDM is that the signal has large amplitude fluctuations caused by the summation of the complex sinusoids. PAPR of OFDM signals increases as the number of subcarriers increases. When high PAPR signals are transmitted through non-linear power amplifier, severe signal distortion will occur. Therefore, highly linear power amplifier with power back off is required for OFDM systems. This results in the low power efficiency and limited battery life of the mobile device. OFDM's high peak to average power ratio (PAPR) requires system components with a large linear range capable of accommodating the signal due to the fact that nonlinear distortion results in a loss of subcarrier orthogonality which degrades performance [6]. Nonlinearities in the transmitter also cause the generation of new frequencies in the transmitted signal. This inter-modulation distortion causes interference among the subcarriers, and a broadening of the overall signal spectrum.

Recently, the idea of constant envelope OFDM with continuous phase modulation (OFDM-CPM) system was introduced [2-5]. The significance of the 0 dB PAPR achieved by using continuous phase modulation (CPM) is that the signal can be amplified with power efficient nonlinear power amplifier. The OFDM-CPM approach described in this paper is based on the phase modulator transform technique. In essence, the OFDM waveform is used to phase modulate the carrier. In [2] and [3], the OFDM-CPM signal-space and performance in AWGN channel was investigated, and a suboptimal phase demodulator receiver was proposed. In [4], a non-coherent receiver was presented for OFDM-CPM in flat fading channels. However, the use of OFDM-CPM has not been evaluated for multipath Stanford University Interim (SUI) channels and under IEEE 802.16 scenario.

SUI multi-path channels are widely used for evaluation of the broadband wireless metropolitan area network (WMAN) systems. WMAN systems are being developed by the IEEE 802.16 working group and also by the European Telecommunications Standards Institute (ETSI) Broadband Radio Access Network (BRAN) High-Performance MAN (Hiper-MAN) group. In this study, these channels are employed to investigate multipath effects on OFDM-CPM under IEEE 802.16 Scenario. This work is going to open a window to use OFDM-CPM in WMANs.

In this paper, the application of OFDM-CPM in multipath SUI channel and under IEEE 802.16 scenario is studied. In this study, performance of the frequency domain equalizer (FDE) using both zero-forcing (ZF) and minimum mean-squared error (MMSE) definitions is evaluated over SUI multipath fading channel models. OFDM-CPM is then compared with conventional 16PSK OFDM in the presence of nonlinear power amplification at 0dB input power back off (IBO). In addition, the effect of the modulation index on the BER performance and spectrum broadening is investigated. For this purpose, simulation results are provided to study the fractional out of band power of OFDM-CPM signals for different modulation indices. Finally, simulation results are provided to investigate the effectiveness of OFDM-CPM phase demodulator receiver for multipath diversity as well as threshold effect at low SNR.

2. OFDM-CPM signal Description

The OFDM-CPM is a modulation format that can be viewed as a mapping of the OFDM signal onto the unit circle. The resulting signal has a constant envelope leading to a 0 dB PAPR. The OFDM signal is transformed through continuous phase modulator to a low-PAPR signal prior to the PA and, at the receiver, the inverse transform by a phase demodulator is performed prior to OFDM demodulation as shown in Fig. 1.

The base band of the OFDM-CPM waveform is represented by:

$$S(t) = e^{j\phi(t)}, \quad (1)$$

where the phase signal during the n th block is written as

$$\phi(t) = \theta_n + 2\pi h C_N \sum_{k=1}^N I_{n,k} q_k(t - nT_B), \quad (2)$$

for $nT_B \leq t < (n+1)T_B$, which is the OFDM waveform plus memory term θ_n . Here h refers to modulation index; N is the number of sub-carriers; $\{I_{n,k}\}$ represents M-PAM data symbols; T_B is the block interval, and $\{q_k(t)\}$ represents the set of subcarrier waveforms. The subcarriers must also be real-valued and $\{q_k(t)\}$ may be expressed as

$$q_k(t) = \begin{cases} \cos(2\pi kt/T_B) & ,0 \leq t < T_B, K \leq N/2 \\ \sin(2\pi(k - N/2)/T_B) & ,0 \leq t < T_B, K > N/2 \\ 0 & ,otherwise \end{cases} \quad (3)$$

The normalizing constant is set to $C_N = (2/N\sigma_I^2)^{-0.5}$, where σ_I^2 is the variance of the data symbols, and consequently the variance of the phase signal will be $\sigma_\phi^2 = (2\pi h)^2$. Assuming that the data is independent and identically distributed, it follows that $\sigma_I^2 = (M^2 - 1)/3$.

To reduce adjacent channel interference, the OFDM-CPM signal is made phase-continuous with the introduction of memory. The benefit of continuous phase OFDM-CPM is a more compact signal spectrum. The phase signal, as defined by (1), has phase jumps at each signalling interval boundary without $\{\theta_n\}$. By including memory terms, these jumps are eliminated. The memory term θ_n , is a function of all data symbols during and prior to the n th signalling interval.

The phase demodulator receiver is a practical implementation of the OFDM-CPM receiver and is therefore of practical interest. However, it isn't necessarily optimum, since the optimum receiver is a bank of M^N matched filters, one for each potentially transmitted signal.

The phase demodulator receiver essentially consists of a phase demodulator followed by a conventional OFDM demodulator. The received signal is first passed through a front-end band pass filter, which limits the bandwidth of the additive noise. [2], [5]

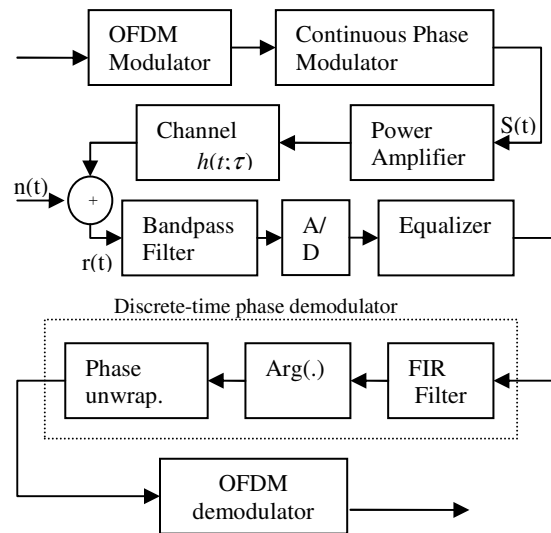


FIGURE 1: OFDM-CPM block diagram.

3. OFDM-CPM in Multipath Channels

In this section, the performance of OFDM-CPM in multipath channels is analysed. In this case, the received signal takes the following form:

$$r(t) = \int_0^{\tau_{\max}} h(t, \tau) S(t - \tau) d\tau + n(t) \quad (3)$$

where $h(t, \tau)$ is the channel impulse response having a maximum propagation delay τ_{\max} and $n(t)$ is complex Gaussian noise. Channel is assumed to be wide-sense stationary uncorrelated scattering (WSSUS), and comprises of L discrete paths. For the proposed system, a cyclic prefix guard interval is transmitted. At the receiver, $r(t)$ is sampled, the guard time samples are discarded and the block time samples are processed. Then frequency domain equalizer is applied. Equalizer correction terms, could be based on ZF or MMSE criterion.

As long as the duration of the guard interval is greater than or equal to the channel's maximum propagation delay, that is, $T_g \gg \tau_{\max}$, and a cyclic prefix is transmitted during the guard interval, the performance of un-coded OFDM in a time-dispersive channel is equivalent to flat fading performance. In other words, the multipath fading performance is the same as single path fading performance. It can be said that OFDM lacks frequency diversity as well. In OFDM the wideband frequency-selective fading channel is converted into N contiguous frequency non-selective fading channels. Therefore any multipath diversity inherent to the channel is not exploited by the OFDM receiver. Note that OFDM systems typically employ channel coding and frequency-domain interleaving, which offers diversity.

Here, Taylor expansion is applied to consider OFDM-CPM behaviour in multipath channels. The OFDM-CPM signal, with $\theta_n = 0$, can be written as

$$S(t) = e^{j\phi(t)} = e^{j\sigma_\phi m(t)} = \sum_{i=0}^{\infty} [(j\sigma_\phi)^i / i!] m^i(t), \quad (4)$$

where $m(t)$ is the normalized OFDM message signal. This can be seen by viewing the OFDM-CPM waveform by the Taylor series expansion

$$S(t) = [1 + j\sigma_\phi m(t) - \frac{\sigma_\phi^2}{2} m^2(t) - j\frac{\sigma_\phi^3}{6} m^3(t) + \dots], \quad (5)$$

for $0 \leq t \leq T_B$, the higher-order terms $m^n(t)$, $n > 1$, results in a frequency spreading of the data symbols. In general, it can be said that the N data symbols that constitute the OFDM-CPM signal are not simply confined to N frequency bins, as is the case with conventional OFDM. The phase modulator mixes and spreads, in a nonlinear and exceedingly complicated manner, the data symbols in frequency, which gives the OFDM-CPM system the potential to exploit the frequency diversity in the channel. These results indicate that the OFDM-CPM receiver exploits the multipath diversity of the channel. The fact that OFDM-CPM exploits multipath diversity is an interesting result since conventional OFDM doesn't. This isn't necessarily the case, however. For small values of modulation index, where only the first two terms in (5) contribute, that is,

$$S(t) = [1 + j\sigma_\phi m(t)] \quad (6)$$

the OFDM-CPM signal doesn't have the frequency spreading given by the higher-order terms. In this case, the OFDM-CPM signal is essentially equivalent to a conventional OFDM signal, $m(t)$, and therefore doesn't have the ability to exploit the frequency diversity of the channel. Simply put, OFDM-CPM has frequency diversity when the modulation index is large and doesn't have frequency diversity when the modulation index is small.

4. Simulation Result

The BER performance of OFDM-CPM is evaluated using computer simulation. In this study, the channel is assumed to be known perfectly at the receiver. The parameters of the representative OFDM-CPM system used for this study are demonstrated in Table 1. These parameters are derived from IEEE802.16 standard [8].

The 256point OFDM based air interface specification seems to be favored by the IEEE 802.16 wireless metropolitan area network (WMAN) standard. The size of the FFT point determines the number of subcarriers. Of these 256 subcarriers, 192 are used for user data, 56 are nulled for guard band and 8 are used as pilot subcarriers for various estimation purposes. The physical layer allows accepting variable CP length of 8, 16, 32 or 64 depending on the expected channel delay spread. The channel bandwidth can be an integer multiple of 1.25 MHz, 1.5 MHz, 1.75 MHz, 2MHz and 2.75 MHz with a maximum of 20 MHz. But the IEEE 802.16 wireless metropolitan area network (WMAN) standard has initially narrowed down the large choice of possible bandwidth to a few possibilities to ensure interoperability between different vendor's products [8].

Here we use SUI channels [7]. The parametric view of the SUI channels is summarized in the Table 2. For each simulation trial, the set of L path gains are generated randomly. Each gain is complex valued, with zero mean and variance $\sigma_{a_i}^2$. Both the real and imaginary parts of the path gains are Gaussian distributed, thus the envelope is Rayleigh distributed. Also, the channels are normalized.

Fig. 2 illustrates OFDM-CPM BER performance over SUI 1-6 channel models for $M=4$ and $2\pi h = 1$. Results on this figure confirm the analysis described in section 3. In addition, this figure compares the SUI 1-6 channels with the AWGN and Rayleigh channels results. As shown in this figure, the performance of the SUI 1-6 channels using MMSE equalizer outperforms the Rayleigh channel performance. For example, in Fig. 2, performance at $\text{BER}=10^{-4}$, over SUI6 is 15 dB better than single path Rayleigh channel.

The results presented in Fig. 2 show that multipath diversity is exploited by the OFDM-CPM phase demodulator receiver as expected from the aforementioned analysis. The multipath diversity depends not only on the number of independent paths but also on the way in which the power is distributed over the paths. It is worth noting that the frequency non-selective channel models considered have $L = 1$ path of which 100% of the channel gain depends, and thus these channels have no multipath diversity. This is the reason that multipath channels outperform Rayleigh channel.

In Fig. 3, the performance of OFDM-CPM with the ZF equalizer and MMSE equalizer over SUI1 and SUI3 is compared. These results show the significant performance improvement provided by using the MMSE equalizer for SUI channels over single path Rayleigh channel. However, these results reveal that for the case of using ZF equalizer, performance in multi path channels could be worse than single path (Rayleigh) channel. At the bit error rate 10^{-4} , for example, MMSE outperforms ZF by 10 dB for Channel SUI1.

In addition, as stated in section 3, OFDM-CPM has frequency diversity when the modulation index is large and doesn't have frequency diversity when the modulation index is small. This property is demonstrated in Fig. 4. It shows the results obtained from simulation of the system over the single path Rayleigh flat fading channel as well as the SUI6 Channel for $M = 4$, $2\pi h = 0.1$ and $2\pi h = 1.1$. As shown in this figure, OFDM-CPM with a small modulation index lacks frequency diversity. Notice that for $2\pi h = 0.1$ the single path and multipath performance is essentially the same. By contrast, for the large modulation index e.g. $2\pi h = 1.1$, the multi-path performance is significantly better than the single-path performance.

On the other hand, the OFDM-CPM power density spectrum $\Phi_s(f)$ can be estimated by the Welch method of periodogram averaging. This estimation can be used to calculate the fractional out-of-band power as follows:

$$FOBP(f) = \frac{\int_0^f \Phi_s(x) dx}{\int_{-\infty}^{+\infty} \Phi_s(f) df}. \quad (7)$$

Fig. 5 compares the estimated fractional out-of-band power curves over a large range of modulation index. As it can be seen in this figure, large amount of modulation index causes spectrum broadening and adjacent channel interference even though it results in better BER performance.

Moreover, in power amplifiers (PA), the most efficient operating point is at the PA's saturation point, but for signals with large PAPR the operating point must shift to the left, keeping the amplification linear. The average input power is reduced and consequently this technique is called input power back-off (IBO). At large back-off the efficiency of a power amplifier is very low. Such efficiency is detrimental to mobile battery-powered devices which have limited power resources. Here we assume that we need $IBO = 0dB$.

Considering the power amplifier nonlinearities, in Fig. 6, the performance of OFDM-CPM is compared with the conventional 16PSK-OFDM over SUI4 channel. In this case $2\pi h = 1$ and $M=16$. In addition, the solid state power amplifier (SSPA) model is employed at 0dB input power back-off level. Here, the advantage of the OFDM-CPM system is that it operates with $IBO = 0dB$. As shown in Fig. 6, over the region $0dB \leq E_b / N_0 \leq 10dB$, the OFDM system performs better than the OFDM-CPM system. Under this 10dB threshold, nonlinear and non-Gaussian noise is injected into the OFDM demodulator (following the phase demodulator) and causes performance degradation.

As a result, this figure reveals that although OFDM-CPM exploits the frequency diversity inherent to the channel, however, OFDM-CPM exhibits a poor performance at low SNR due to the threshold effect.

5. CONCLUSION

In this paper, application of OFDM-CPM for SUI multipath channels is analyzed. The results obtained show that OFDM-CPM exploits the frequency diversity of the multipath channel. This diversity comes from spreading of the data symbol energy in frequency-domain for large modulation index. For small modulation index, however, OFDM-CPM does not achieve diversity gains. This phenomenon is explained by viewing the OFDM-CPM signal in its Taylor expanded form. On the other hand, large amount of modulation index causes spectrum broadening and adjacent channel interference even though it results in better BER performance. In addition, OFDM-CPM is compared with conventional 16PSK OFDM in the presence of nonlinear power amplification at 0dB input power back-off (IBO). Taking into account the IBO, OFDM-CPM is shown to outperform OFDM at high bit energy to-noise density ratios (E_b/N_0). However, at low SNR the OFDM-CPM phase demodulator receiver suffers from a threshold effect.

TABLE 1: System and Signal parameters

T_B	Block Interval	114 μ s		
T_g	Guard Interval	32 μ s		
T_F	Frame Interval	146 μ s		
J	Oversampling Factor	8		
$F_{sa} = JN_B / T_B$	Sampling Frequency	14Mega (samp./sec)		
N_B	N_g	N_F	Num. of Carriers	200 56 256
$BW = N / T_B$		Bandwidth	1.75MHz	
η_t	Transmission efficiency	114/146 = %78		
$1/T_B$	Subcarrier Spacing	8750Hz		

TABLE 2: SUI Channel Parameters

Model	Delay	L (Num of Taps) = 3			Delay spread (τ_{rms})
	Gain	Tap1	Tap2	Tap3	
SUI 1	0 μ s	0.4 μ s	0.8 μ s	0.111 μ s	
	0dB	-15dB	-20dB		
SUI 2	0 μ s	0.5 μ s	1 μ s	0.202 μ s	
	0dB	-12dB	-15dB		
SUI 3	0 μ s	0.5 μ s	1 μ s	0.264 μ s	
	0dB	-5dB	-10dB		
SUI 4	0 μ s	2 μ s	4 μ s	1.257 μ s	
	0dB	-4dB	-8dB		
SUI 5	0 μ s	5 μ s	10 μ s	2.842 μ s	
	0dB	-5dB	-10dB		
SUI 6	0 μ s	14 μ s	20 μ s	5.240 μ s	
	0dB	-10dB	-14dB		

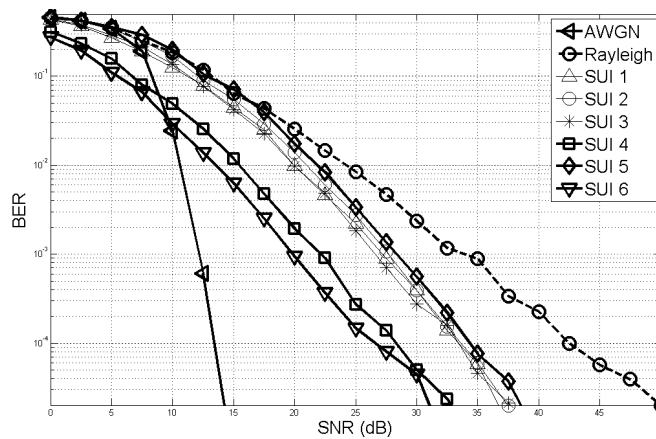


FIGURE 2: OFDM-CPM Performance Simulation (M=4, N=256, MMSE)

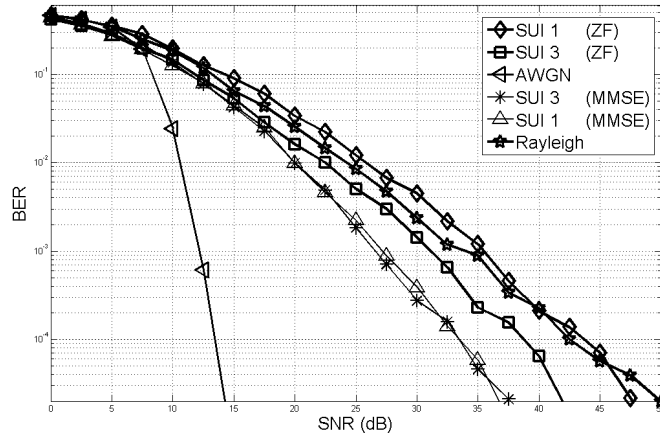


FIGURE 3: Performance Simulation (ZF and MMSE)

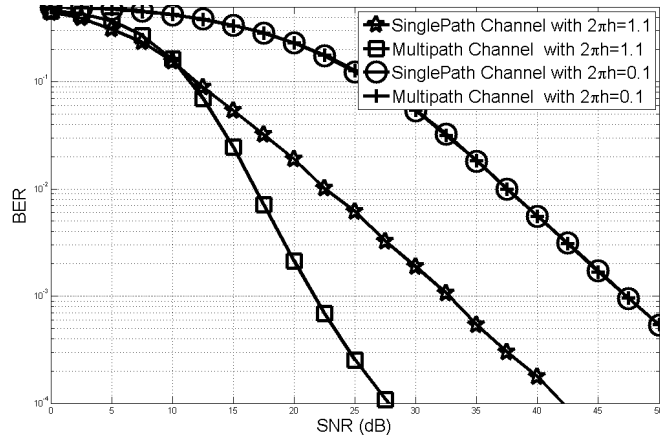


FIGURE 4: Performance Simulation (Modulation index effect)

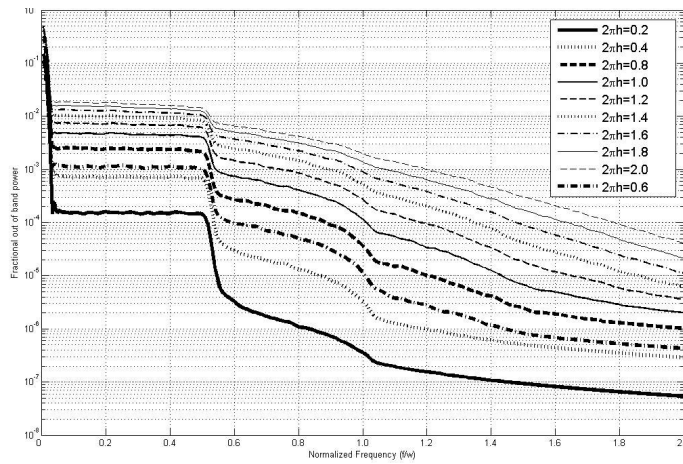


FIGURE 5: Fractional out of band power Simulation (Modulation index effect)

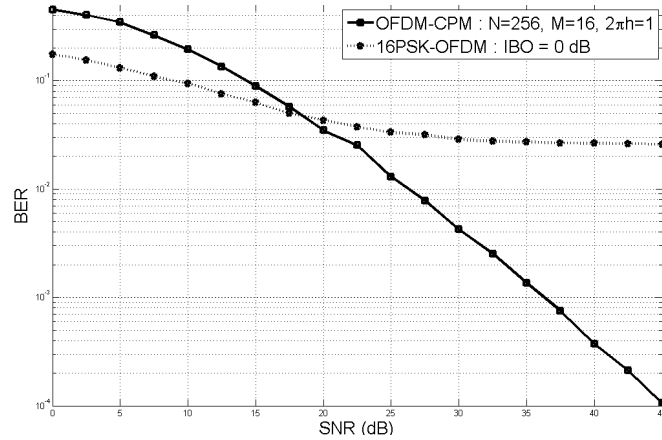


FIGURE 6: Performance Simulation (OFDM-CPM and 16PSK-OFDM)

REFERENCES

1. Z. Wang, Xiaoli Ma, and G. B. Giannakis. "OFDM or Single-Carrier Block Transmissions?" IEEE Transaction on Communications, 25(3):36-44, 2004
2. S. C. Thompson, J. G. Proakis, and J. R. Zeidler. "Constant envelope binary OFDM phase modulation". In Proceedings of the 23rd Military Communication Conference. Baltimore, MD, USA, 2003
3. S. C. Thompson, A. U. Ahmed, J. G. Proakis, and J. R. Zeidler. "Constant envelope OFDM phase modulation: spectral containment, signal space properties and performance". In Proceedings of the 23rd Military Communication Conference. Baltimore, MD, USA, 2004
4. Tsai, G. Zhang, and J. L. Pan. "Orthogonal frequency division multiplexing with phase modulation and constant envelope design". In Proceedings of the 23rd Military Communication Conference. Baltimore, MD, USA, 2005
5. S. C. Thompson, J. G. Proakis, and J. R. Zeidler. "Noncoherent Reception of Constant Envelope OFDM in Flat Fading Channels". In Proceedings of the IEEE 16th International Symposium on PIMRC. Baltimore, MD, USA, 2005
6. S. C. Thompson, J. G. Proakis, and J. R. Zeidler. "The effectiveness of signal clipping for PAPR and total degradation reduction in OFDM systems". In Proceedings of the IEEE 16th GLOBECOM. Baltimore, MD, USA, 2005
7. V. Erceg, K.V.S. Hari, M.S. Smith, D.S. Baum et al, "Channel Models for Fixed Wireless Applications", IEEE 802.16.3 Task Group Contributions, Feb2003
8. IEEE 802.16 2004," IEEE Standard for Local and Metropolitan Area Networks Part16: Air Interface for Fixed Broadband Wireless Access Systems", 1 October 2004

COMPUTER SCIENCE JOURNALS SDN BHD
M-3-19, PLAZA DAMAS
SRI HARTAMAS
50480, KUALA LUMPUR
MALAYSIA